

US EPA ARCHIVE DOCUMENT

**USER'S GUIDE FOR THE INDUSTRIAL
SOURCE COMPLEX (ISC3) DISPERSION
MODELS FOR USE IN THE MULTIMEDIA,
MULTIPATHWAY AND MULTIRECEPTOR
RISK ASSESSMENT (3MRA) FOR HWIR99**

**VOLUME II: DESCRIPTION OF MODEL
ALGORITHMS**

DRAFT

Work Assignment Manager
and Technical Direction:

Donna B. Schwede
U.S. Environmental Protection Agency
Office of Research and Development
Research Triangle Park, NC 27711

Prepared by:

Pacific Environmental Services
5001 South Miami Boulevard, Suite 300
P.O. Box 12077
Research Triangle Park, NC 27709-2077
Under Contract No. 68-D7-0002 WA 1-001

U.S. Environmental Protection Agency
Office of Solid Waste
Washington, DC 20460

June 30, 1999

DISCLAIMER

The information in this document has been reviewed in its entirety by the U.S. Environmental Protection Agency (EPA), and approved for publication as an EPA document. Mention of trade names, products, or services does not convey, and should not be interpreted as conveying official EPA endorsement, or recommendation.

PREFACE

This User's Guide provides documentation for the Industrial Source Complex (ISC3) models, referred to hereafter as the Short Term (ISCST3) and Long Term (ISCLT3) models. This volume describes the dispersion algorithms utilized in the ISCST3 and ISCLT3 models, including the new area source and dry deposition algorithms, both of which are a part of Supplement C to the Guideline on Air Quality Models (Revised).

This volume also includes a technical description for the following algorithms that are not included in Supplement C: pit retention (ISCST3 and ISCLT3), wet deposition (ISCST3 only), and COMPLEX1 (ISCST3 only). The pit retention and wet deposition algorithms have not undergone extensive evaluation at this time, and their use is optional. COMPLEX1 is incorporated to provide a means for conducting screening estimates in complex terrain. EPA guidance on complex terrain screening procedures is provided in Section 5.2.1 of the Guideline on Air Quality Models (Revised).

Volume I of the ISC3 User's Guide provides user instructions for the ISC3 models.

ACKNOWLEDGEMENTS

The User's Guide for the ISC3 Models has been prepared by Pacific Environmental Services, Inc., Research Triangle Park, North Carolina. This effort has been funded by the Environmental Protection Agency (EPA) under Contract No. 68-D30032, with Desmond T. Bailey as Work Assignment Manager (WAM). The technical description for the dry deposition algorithm was developed from material prepared by Sigma Research Corporation and funded by EPA under Contract No. 68-D90067, with Jawad S. Touma as WAM.

CONTENTS

PREFACE	iii
ACKNOWLEDGEMENTS	iv
FIGURES	vii
TABLES	viii
SYMBOLS	ix
1.0 THE ISC SHORT-TERM DISPERSION MODEL EQUATIONS	1-1
1.1 POINT SOURCE EMISSIONS	1-2
1.1.1 The Gaussian Equation	1-2
1.1.2 Downwind and Crosswind Distances	1-3
1.1.3 Wind Speed Profile	1-4
1.1.4 Plume Rise Formulas	1-5
1.1.5 The Dispersion Parameters	1-15
1.1.6 The Vertical Term	1-31
1.1.7 The Decay Term	1-39
1.2 NON-POINT SOURCE EMISSIONS	1-40
1.2.1 General	1-40
1.2.2 The Short-Term Volume Source Model	1-41
1.2.3 The Short-Term Area Source Model	1-44
1.2.4 The Short-Term Open Pit Source Model	1-48
1.3 THE ISC SHORT-TERM DRY DEPOSITION MODEL	1-53
1.3.1 General	1-53
1.3.2 Deposition and Gravitational Settling Velocities	1-54
1.3.3 Point and Volume Source Emissions	1-59
1.3.4 Area and Open Pit Source Emissions	1-60
1.4 THE ISC SHORT-TERM WET DEPOSITION MODEL	1-61
1.5 ISC COMPLEX TERRAIN SCREENING ALGORITHMS	1-63
1.5.1 The Gaussian Sector Average Equation	1-63
1.5.2 Downwind, Crosswind and Radial Distances	1-65
1.5.3 Wind Speed Profile	1-65
1.5.4 Plume Rise Formulas	1-65
1.5.5 The Dispersion Parameters	1-66
1.5.6 The Vertical Term	1-67
1.5.7 The Decay Term	1-69
1.5.8 The Plume Attenuation Correction Factor	1-69
1.5.9 Wet Deposition in Complex Terrain	1-72
1.6 ISC TREATMENT OF INTERMEDIATE TERRAIN	1-72
2.0 THE ISC LONG-TERM DISPERSION MODEL EQUATIONS	2-1

2.1 POINT SOURCE EMISSIONS 2-1

 2.1.1 The Gaussian Sector Average Equation 2-1

 2.1.2 Downwind and Crosswind Distances 2-4

 2.1.3 Wind Speed Profile 2-4

 2.1.4 Plume Rise Formulas 2-4

 2.1.5 The Dispersion Parameters 2-4

 2.1.6 The Vertical Term 2-6

 2.1.7 The Decay Term 2-7

 2.1.8 The Smoothing Function 2-7

2.2 NON-POINT SOURCE EMISSIONS 2-8

 2.2.1 General 2-8

 2.2.2 The Long-Term Volume Source Model 2-8

 2.2.3 The Long-Term Area Source Model 2-9

 2.2.4 The Long-Term Open Pit Source Model 2-12

2.3 THE ISC LONG-TERM DRY DEPOSITION MODEL 2-12

 2.3.1 General 2-12

 2.3.2 Point and Volume Source Emissions 2-13

 2.3.3 Area and Open Pit Source Emissions 2-14

3.0 REFERENCES 3-1

INDEX INDEX-1

FIGURES

<u>Figure</u>	<u>Page</u>
1-1 LINEAR DECAY FACTOR, A AS A FUNCTION OF EFFECTIVE STACK HEIGHT, H_e . A SQUAT BUILDING IS ASSUMED FOR SIMPLICITY.	1-71
1-2 ILLUSTRATION OF TWO TIERED BUILDING WITH DIFFERENT TIERS DOMINATING DIFFERENT WIND DIRECTIONS	1-72
1-3 THE METHOD OF MULTIPLE PLUME IMAGES USED TO SIMULATE PLUME REFLECTION IN THE ISC MODEL	1-73
1-4 SCHEMATIC ILLUSTRATION OF MIXING HEIGHT INTERPOLATION PROCEDURES	1-74
1-5 ILLUSTRATION OF PLUME BEHAVIOR IN COMPLEX TERRAIN ASSUMED BY THE ISC MODEL	1-75
1-6 ILLUSTRATION OF THE DEPLETION FACTOR F_0 AND THE CORRESPONDING PROFILE CORRECTION FACTOR $P(x,z)$. . .	1-76
1-7 VERTICAL PROFILE OF CONCENTRATION BEFORE AND AFTER APPLYING F_0 AND $P(x,z)$ SHOWN IN FIGURE 1-6	1-77
1-8 EXACT AND APPROXIMATE REPRESENTATION OF LINE SOURCE BY MULTIPLE VOLUME SOURCES	1-78
1-9 REPRESENTATION OF AN IRREGULARLY SHAPED AREA SOURCE BY 4 RECTANGULAR AREA SOURCES	1-79
1-10 EFFECTIVE AREA AND ALONGWIND LENGTH FOR AN OPEN PIT SOURCE	1-80
1-11 WET SCAVENGING RATE COEFFICIENT AS A FUNCTION OF PARTICLE SIZE (JINDAL & HEINOLD, 1991)	1-81

TABLES

<u>Table</u>	<u>Page</u>
PARAMETERS USED TO CALCULATE PASQUILL-GIFFORD F_y	1-16
PARAMETERS USED TO CALCULATE PASQUILL-GIFFORD F_z	1-17
BRIGGS FORMULAS USED TO CALCULATE McELROY-POOLER F_y	1-19
BRIGGS FORMULAS USED TO CALCULATE McELROY-POOLER F_z	1-19
COEFFICIENTS USED TO CALCULATE LATERAL VIRTUAL DISTANCES FOR PASQUILL-GIFFORD DISPERSION RATES	1-21
SUMMARY OF SUGGESTED PROCEDURES FOR ESTIMATING INITIAL LATERAL DIMENSIONS F_{y_0} AND INITIAL VERTICAL DIMENSIONS F_{z_0} FOR VOLUME AND LINE SOURCES	43

SYMBOLS

<u>Symbol</u>	<u>Definition</u>
A	Linear decay term for vertical dispersion in Schulman-Scire downwash (dimensionless)
A_e	Effective area for open pit emissions (dimensionless)
D	Exponential decay term for Gaussian plume equation (dimensionless)
D_B	Brownian diffusivity (cm/s)
D_r	Relative pit depth (dimensionless)
d_e	Effective pit depth (m)
d_p	Particle diameter for particulate emissions (:m)
d_s	Stack inside diameter (m)
F_b	Buoyancy flux parameter (m^4/s^3)
F_d	Dry deposition flux (g/m^2)
F_m	Momentum flux parameter (m^4/s^2)
F_Q	Plume depletion factor for dry deposition (dimensionless)
F_T	Terrain adjustment factor (dimensionless)
F_w	Wet deposition flux (g/m^2)
f	Frequency of occurrence of a wind speed and stability category combination (dimensionless)
g	Acceleration due to gravity ($9.80616 m/s^2$)
h_b	Building height (m)
h_e	Plume (or effective stack) height (m)
h_s	Physical stack height (m)

h_{ter}	Height of terrain above stack base (m)
h_s'	Release height modified for stack-tip downwash (m)
h_w	Crosswind projected width of building adjacent to a stack (m)
k	von Karman constant (= 0.4)
L	Monin-Obukhov length (m)
L_y	Initial plume length for Schulman-Scire downwash sources with enhanced lateral plume spread (m)
L_b	Lesser of the building height and crosswind projected building width (m)
R	Alongwind length of open pit source (m)
$P(x,y)$	Profile adjustment factor (dimensionless)
p	Wind speed power law profile exponent (dimensionless)
Q_A	Area Source pollutant emission rate (g/s)
Q_e	Effective emission rate for effective area source for an open pit source (g/s)
Q_i	Adjusted emission rate for particle size category for open pit emissions (g/s)
Q_s	Pollutant emission rate (g/s)
Q_J	Total amount of pollutant emitted during time period J (g)
R	Precipitation rate (mm/hr)
R_o	Initial plume radius for Schulman-Scire downwash sources (m)
$R(z, z_d)$	Atmospheric resistance to vertical transport (s/cm)
r	Radial distance range in a polar receptor network (m)

r_a	Atmospheric resistance (s/cm)
r_d	Deposition layer resistance (s/cm)
s	Stability parameter = $g \frac{\partial \theta / \partial z}{T_a}$
S	Smoothing term for smoothing across adjacent sectors in the Long Term model (dimensionless)
S_{CF}	Slip correction factor (dimensionless)
Sc	Schmidt number = ν / D_p (dimensionless)
St	Stokes number = $(v_g / g) (u_*^2 / \nu)$ (dimensionless)
T_a	Ambient temperature (K)
T_s	Stack gas exit temperature (K)
u_{ref}	Wind speed measured at reference anemometer height (m/s)
u_s	Wind speed adjusted to release height (m/s)
u_*	Surface friction velocity (m/s)
V	Vertical term of the Gaussian plume equation (dimensionless)
V_d	Vertical term with dry deposition of the Gaussian plume equation (dimensionless)
v_d	Particle deposition velocity (cm/s)
v_g	Gravitational settling velocity for particles (cm/s)
v_s	Stack gas exit velocity (m/s)
X	X-coordinate in a Cartesian grid receptor network (m)
x_o	Length of side of square area source (m)
Y	Y-coordinate in a Cartesian grid receptor network (m)

- 2** Direction in a polar receptor network (degrees)
- x Downwind distance from source to receptor (m)
- x_y Lateral virtual point source distance (m)
- x_z Vertical virtual point source distance (m)
- x_f Downwind distance to final plume rise (m)
- x^* Downwind distance at which turbulence dominates entrainment (m)
- y Crosswind distance from source to receptor (m)
- z Receptor/terrain height above mean sea level (m)
- z_d Dry deposition reference height (m)
- z_r Receptor height above ground level (i.e. flagpole) (m)
- z_{ref} Reference height for wind speed power law (m)
- z_s Stack base elevation above mean sea level (m)
- z_i Mixing height (m)
- z_0 Surface roughness height (m)
- $\$$ Entrainment coefficient used in buoyant rise for Schulman-Scire downwash sources = 0.6
- $\$_j$ Jet entrainment coefficient used in gradual momentum plume rise calculations = $\frac{1}{3} + \frac{u_s}{v_s}$
-)h Plume rise (m)
- M2/Mz Potential temperature gradient with height (K/m)
- g_i Escape fraction of particle size category for open pit emissions (dimensionless)
- 7** Precipitation scavenging ratio (s^{-1})

- 8** Precipitation rate coefficient (s-mm/hr)⁻¹
- B** pi = 3.14159
- R** Decay coefficient = 0.693/T_{1/2} (s⁻¹)
- R_H** Stability adjustment factor (dimensionless)
- N** Fraction of mass in a particular settling velocity category for particulates (dimensionless)
- D** Particle density (g/cm³)
- D_{AIR}** Density of air (g/cm³)
- F_Y** Horizontal (lateral) dispersion parameter (m)
- F_{yo}** Initial horizontal dispersion parameter for virtual point source (m)
- F_{ye}** Effective lateral dispersion parameter including effects of buoyancy-induced dispersion (m)
- F_z** Vertical dispersion parameter (m)
- F_{zo}** Initial vertical dispersion parameter for virtual point source (m)
- F_{ze}** Effective vertical dispersion parameter including effects of buoyancy-induced dispersion (m)
- L** Viscosity of air • 0.15 cm²/s
- :** Absolute viscosity of air • 1.81 x 10⁻⁴ g/cm/s
- P** Concentration (:g/m³)
- P_d** Concentration with dry deposition effects (:g/m³)

1.0 THE ISC SHORT-TERM DISPERSION MODEL EQUATIONS

The Industrial Source Complex (ISC) Short Term model provides options to model emissions from a wide range of sources that might be present at a typical industrial source complex. The basis of the model is the straight-line, steady-state Gaussian plume equation, which is used with some modifications to model simple point source emissions from stacks, emissions from stacks that experience the effects of aerodynamic downwash due to nearby buildings, isolated vents, multiple vents, storage piles, conveyor belts, and the like. Emission sources are categorized into four basic types of sources, i.e., point sources, volume sources, area sources, and open pit sources. The volume source option and the area source option may also be used to simulate line sources. The algorithms used to model each of these source types are described in detail in the following sections. The point source algorithms are described in Section 1.1. The volume, area and open pit source model algorithms are described in Section 1.2. Section 1.3 gives the optional algorithms for calculating dry deposition for point, volume, area and open pit sources, and Section 1.4 describes the optional algorithms for calculating wet deposition. Sections 1.1 through 1.4 describe calculations for simple terrain (defined as terrain elevations below the release height). The modifications to these calculations to account for complex terrain are described in Section 1.5, and the treatment of intermediate terrain is discussed in Section 1.6.

The ISC Short Term model accepts hourly meteorological data records to define the conditions for plume rise, transport, diffusion, and deposition. The model estimates the concentration or deposition value for each source and receptor

combination for each hour of input meteorology, and calculates user-selected short-term averages. For deposition values, either the dry deposition flux, the wet deposition flux, or the total deposition flux may be estimated. The total deposition flux is simply the sum of the dry and wet deposition fluxes at a particular receptor location. The user also has the option of selecting averages for the entire period of input meteorology.

1.1 POINT SOURCE EMISSIONS

The ISC Short Term model uses a steady-state Gaussian plume equation to model emissions from point sources, such as stacks and isolated vents. This section describes the Gaussian point source model, including the basic Gaussian equation, the plume rise formulas, and the formulas used for determining dispersion parameters.

1.1.1 The Gaussian Equation

The ISC short term model for stacks uses the steady-state Gaussian plume equation for a continuous elevated source. For each source and each hour, the origin of the source's coordinate system is placed at the ground surface at the base of the stack. The x axis is positive in the downwind direction, the y axis is crosswind (normal) to the x axis and the z axis extends vertically. The fixed receptor locations are converted to each source's coordinate system for each hourly concentration calculation. The calculation of the downwind and crosswind distances is described in Section 1.1.2. The hourly concentrations calculated for each source at each receptor are summed to obtain the total concentration produced at each receptor by the combined source emissions.

For a steady-state Gaussian plume, the hourly concentration at downwind distance x (meters) and crosswind distance y (meters) is given by:

$$C = \frac{QKVD}{2\pi u_s \sigma_y \sigma_z} \exp\left[-0.5\left(\frac{y}{\sigma_y}\right)^2\right] \quad (1-1)$$

where:

- Q = pollutant emission rate (mass per unit time)
- K = a scaling coefficient to convert calculated concentrations to desired units (default value of 1×10^6 for Q in g/s and concentration in :g/m³)
- V = vertical term (See Section 1.1.6)
- D = decay term (See Section 1.1.7)
- F_y, F_z = standard deviation of lateral and vertical concentration distribution (m) (See Section 1.1.5)
- u_s = mean wind speed (m/s) at release height (See Section 1.1.3)

Equation (1-1) includes a Vertical Term (V), a Decay Term (D), and dispersion parameters (F_y and F_z) as discussed below. It should be noted that the Vertical Term includes the effects of source elevation, receptor elevation, plume rise, limited mixing in the vertical, and the gravitational settling and dry deposition of particulates (with diameters greater than about 0.1 microns).

1.1.2 Downwind and Crosswind Distances

The ISC model uses either a polar or a Cartesian receptor network as specified by the user. The model allows for the use of both types of receptors and for multiple networks in a

single run. All receptor points are converted to Cartesian (X,Y) coordinates prior to performing the dispersion calculations. In the polar coordinate system, the radial coordinate of the point (r, θ) is measured from the user-specified origin and the angular coordinate θ is measured clockwise from the north. In the Cartesian coordinate system, the X axis is positive to the east of the user-specified origin and the Y axis is positive to the north. For either type of receptor network, the user must define the location of each source with respect to the origin of the grid using Cartesian coordinates. In the polar coordinate system, assuming the origin is at $X = X_0$, $Y = Y_0$, the X and Y coordinates of a receptor at the point (r, θ) are given by:

$$X(R) = r \sin \theta - X_0 \quad (1-2)$$

$$Y(R) = r \cos \theta - Y_0 \quad (1-3)$$

If the X and Y coordinates of the source are X(S) and Y(S), the downwind distance x to the receptor, along the direction of plume travel, is given by:

$$x = -(X(R) - X(S)) \sin(WD) - (Y(R) - Y(S)) \cos(WD) \quad (1-4)$$

where WD is the direction from which the wind is blowing. The downwind distance is used in calculating the distance-dependent plume rise (see Section 1.1.4) and the dispersion parameters (see Section 1.1.5). If any receptor is located within 1 meter of a point source or within 1 meter of the effective radius of a volume source, a warning message is printed and no concentrations are calculated for the source-receptor

combination. The crosswind distance y to the receptor from the plume centerline is given by:

$$r = (X(R) - X(S)) \cos(WD) - (Y(R) - Y(S)) \sin(WD) \tag{1-5}$$

The crosswind distance is used in Equation (1-1).

1.1.3 Wind Speed Profile

The wind power law is used to adjust the observed wind speed, u_{ref} , from a reference measurement height, z_{ref} , to the stack or release height, h_s . The stack height wind speed, u_s , is used in the Gaussian plume equation (Equation 1-1), and in the plume rise formulas described in Section 1.1.4. The power law equation is of the form:

$$u_s = u_{ref} \left(\frac{h_s}{z_{ref}} \right)^p \tag{1-6}$$

where p is the wind profile exponent. Values of p may be provided by the user as a function of stability category and wind speed class. Default values are as follows:

Stability Category	Rural Exponent	Urban Exponent
A	0.07	0.15
B	0.07	0.15
C	0.10	0.20
D	0.15	0.25
E	0.35	0.30
F	0.55	0.30

The stack height wind speed, u_s , is not allowed to be less than 1.0 m/s.

1.1.4 Plume Rise Formulas

The plume height is used in the calculation of the Vertical Term described in Section 1.1.6. The Briggs plume rise equations are discussed below. The description follows Appendix B of the Addendum to the MPTER User's Guide (Chico and Catalano, 1986) for plumes unaffected by building wakes. The distance dependent momentum plume rise equations, as described in (Bowers, et al., 1979), are used to determine if the plume is affected by the wake region for building downwash calculations. These plume rise calculations for wake determination are made assuming no stack-tip downwash for both the Huber-Snyder and the Schulman-Scire methods. When the model executes the building downwash methods of Schulman and Scire, the reduced plume rise suggestions of Schulman and Scire (1980) are used, as described in Section 1.1.4.11.

1.1.4.1 Stack-tip Downwash.

In order to consider stack-tip downwash, modification of the physical stack height is performed following Briggs (1974, p. 4). The modified physical stack height h_s' is found from:

$$h_s' = h_s + 2d_s \left| \frac{v_s}{u_s} - 1.5 \right| \quad \text{for } v_s < 1.5u_s \quad (1-7)$$

$$h_s' = h_s \quad \text{for } v_s \geq 1.5u_s$$

where h_s is physical stack height (m), v_s is stack gas exit velocity (m/s), and d_s is inside stack top diameter (m). This h_s' is used throughout the remainder of the plume height

computation. If stack tip downwash is not considered, $h_s' = h_s$ in the following equations.

1.1.4.2 Buoyancy and Momentum Fluxes.

For most plume rise situations, the value of the Briggs buoyancy flux parameter, F_b (m^4/s^3), is needed. The following equation is equivalent to Equation (12), (Briggs, 1975, p. 63):

$$F_b = g v_s d_s^2 \left(\frac{\Delta T}{4 T_s} \right) \tag{1-8}$$

where $\Delta T = T_s - T_a$, T_s is stack gas temperature (K), and T_a is ambient air temperature (K).

For determining plume rise due to the momentum of the plume, the momentum flux parameter, F_m (m^4/s^2), is calculated based on the following formula:

$$F_m = v_s^2 d_s^2 \frac{T_a}{4 T_s} \tag{1-9}$$

1.1.4.3 Unstable or Neutral - Crossover Between Momentum and Buoyancy.

For cases with stack gas temperature greater than or equal to ambient temperature, it must be determined whether the plume rise is dominated by momentum or buoyancy. The crossover temperature difference, $(\Delta T)_c$, is determined by setting Briggs' (1969, p. 59) Equation 5.2 equal to the combination of Briggs' (1971, p. 1031) Equations 6 and 7, and solving for ΔT , as follows:

for $F_b < 55$,

$$(\Delta T)_c = 0.0297 T_s \frac{v_s^{1/3}}{d_s^{2/3}} \tag{1-10}$$

and for $F_b \geq 55$,

$$(\Delta T)_c = 0.00575 T_s \frac{V_s^{2/3}}{d_s^{1/3}} \quad (1-11)$$

If the difference between stack gas and ambient temperature, (ΔT) , exceeds or equals $(\Delta T)_c$, plume rise is assumed to be buoyancy dominated, otherwise plume rise is assumed to be momentum dominated.

1.1.4.4 Unstable or Neutral - Buoyancy Rise.

For situations where (ΔT) exceeds $(\Delta T)_c$ as determined above, buoyancy is assumed to dominate. The distance to final rise, x_f , is determined from the equivalent of Equation (7), (Briggs, 1971, p. 1031), and the distance to final rise is assumed to be $3.5x^*$, where x^* is the distance at which atmospheric turbulence begins to dominate entrainment. The value of x_f is calculated as follows:

for $F_b < 55$:

$$x_f = 49 F_b^{5/8} \quad (1-12)$$

and for $F_b \geq 55$:

$$x_f = 119 F_b^{2/5} \quad (1-13)$$

The final effective plume height, h_e (m), is determined from the equivalent of the combination of Equations (6) and (7) (Briggs, 1971, p. 1031):

for $F_b < 55$:

$$h_e = h_s' + 21.425 \frac{F_b^{3/4}}{u_s} \quad (1-14)$$

and for $F_b \leq 55$:

$$h_e = h_s' + 38.71 \frac{F_b^{3/5}}{u_s} \quad (1-15)$$

1.1.4.5 Unstable or Neutral - Momentum Rise.

For situations where the stack gas temperature is less than or equal to the ambient air temperature, the assumption is made that the plume rise is dominated by momentum. If $(T)_{\text{stack}}$ is less than $(T)_{\text{ambient}}$ from Equation (1-10) or (1-11), the assumption is also made that the plume rise is dominated by momentum. The plume height is calculated from Equation (5.2) (Briggs, 1969, p. 59):

$$h_e = h_s' + 3d_s \frac{v_s}{u_s} \quad (1-16)$$

Briggs (1969, p. 59) suggests that this equation is most applicable when v_s/u_s is greater than 4.

1.1.4.6 Stability Parameter.

For stable situations, the stability parameter, s , is calculated from the Equation (Briggs, 1971, p. 1031):

$$s = g \frac{\partial \theta / \partial z}{T_a} \quad (1-17)$$

As a default approximation, for stability class E (or 5) $\Delta T / \Delta z$ is taken as 0.020 K/m, and for class F (or 6), $\Delta T / \Delta z$ is taken as 0.035 K/m.

1.1.4.7 Stable - Crossover Between Momentum and Buoyancy.

For cases with stack gas temperature greater than or equal to ambient temperature, it must be determined whether the plume rise is dominated by momentum or buoyancy. The crossover temperature difference, $(\Delta T)_c$, is determined by setting Briggs' (1975, p. 96) Equation 59 equal to Briggs' (1969, p. 59) Equation 4.28, and solving for ΔT , as follows:

$$(\Delta T)_c = 0.019582 T_s v_s \sqrt{s} \quad (1-18)$$

If the difference between stack gas and ambient temperature, ΔT , exceeds or equals $(\Delta T)_c$, plume rise is assumed to be buoyancy dominated, otherwise plume rise is assumed to be momentum dominated.

1.1.4.8 Stable - Buoyancy Rise.

For situations where ΔT exceeds $(\Delta T)_c$ as determined above, buoyancy is assumed to dominate. The distance to final rise, x_f , is determined by the equivalent of a combination of Equations (48) and (59) in Briggs, (1975), p. 96:

$$x_f = 2.0715 \frac{u_s}{\sqrt{s}} \quad (1-19)$$

The plume height, h_e , is determined by the equivalent of Equation (59) (Briggs, 1975, p. 96):

$$h_e = h_s' + 2.6 \left(\frac{F_b}{u_s s} \right)^{1/3} \quad (1-20)$$

1.1.4.9 Stable - Momentum Rise.

Where the stack gas temperature is less than or equal to the ambient air temperature, the assumption is made that the plume rise is dominated by momentum. If (T) is less than $(T)_c$ as determined by Equation (1-18), the assumption is also made that the plume rise is dominated by momentum. The plume height is calculated from Equation 4.28 of Briggs ((1969), p. 59):

$$h_e = h_s' + 1.5 \left(\frac{F_m}{u_s \sqrt{S}} \right)^{1/3} \quad (1-21)$$

The equation for unstable-neutral momentum rise (1-16) is also evaluated. The lower result of these two equations is used as the resulting plume height, since stable plume rise should not exceed unstable-neutral plume rise.

1.1.4.10 All Conditions - Distance Less Than Distance to Final Rise.

Where gradual rise is to be estimated for unstable, neutral, or stable conditions, if the distance downwind from source to receptor, x , is less than the distance to final rise, the equivalent of Equation 2 of Briggs ((1972), p. 1030) is used to determine plume height:

$$h_e = h_s' + 1.60 \left(\frac{F_b^{1/3} X^{2/3}}{u_s} \right) \quad (1-22)$$

This height will be used only for buoyancy dominated conditions; should it exceed the final rise for the appropriate condition, the final rise is substituted instead.

For momentum dominated conditions, the following equations (Bowers, et al, 1979) are used to calculate a distance dependent momentum plume rise:

a) unstable conditions:

$$h_e = h_s' + \left(\frac{3F_m x}{\beta_j^2 u_s^2} \right)^{1/3} \quad (1-23)$$

where x is the downwind distance (meters), with a maximum value defined by x_{\max} as follows:

$$\begin{aligned} x_{\max} &= \frac{4d_s (v_s + 3u_s)^2}{v_s u_s} && \text{for } F_b = 0 \\ &= 49F_b^{5/6} && \text{for } 0 < F_b \leq 55\text{m}^4/\text{s}^3 \\ &= 119F_b^{2/5} && \text{for } F_b > 55\text{m}^4/\text{s}^3 \end{aligned} \quad (1-24)$$

b) stable conditions:

$$h_e = h_s' + \left[3F_m \frac{\sin(x\sqrt{s}/u_s)}{\beta_j^2 u_s \sqrt{s}} \right]^{1/3} \quad (1-25)$$

where x is the downwind distance (meters), with a maximum value defined by x_{\max} as follows:

$$x_{\max} = 0.5 \frac{\pi u_s}{\sqrt{s}} \quad (1-26)$$

The jet entrainment coefficient, S_j , is given by,

$$\beta_j = \frac{1}{3} + \frac{u_s}{v_s} \quad (1-27)$$

As with the buoyant gradual rise, if the distance-dependent momentum rise exceeds the final rise for the appropriate condition, then the final rise is substituted instead.

1.1.4.10.1 Calculating the plume height for wake effects determination.

The building downwash algorithms in the ISC models always require the calculation of a distance dependent momentum plume rise. When building downwash is being simulated, the equations described above are used to calculate a distance dependent momentum plume rise at a distance of two building heights downwind from the leeward edge of the building. However, stack-tip downwash is not used when performing this calculation (i.e. $h_s' = h_s$). This wake plume height is compared to the wake height based on the good engineering practice (GEP) formula to determine whether the building wake effects apply to the plume for that hour.

The procedures used to account for the effects of building downwash are discussed more fully in Section 1.1.5.3. The plume rise calculations used with the Schulman-Scire algorithm are discussed in Section 1.1.4.11.

1.1.4.11 Plume Rise When Schulman and Scire Building Downwash is Selected.

The Schulman-Scire downwash algorithms are used by the ISC models when the stack height is less than the building height plus one half of the lesser of the building height or width. When these criteria are met, the ISC models estimate plume rise during building downwash conditions following the suggestion of Scire and Schulman (1980). The plume rise during building

downwash conditions is reduced due to the initial dilution of the plume with ambient air.

The plume rise is estimated as follows. The initial dimensions of the downwashed plume are approximated by a line source of length L_y and depth $2R_o$ where:

$$R_o = \sqrt{2A}\sigma_z \quad x = 3L_B \quad (1-28)$$

$$L_y = \sqrt{2\Pi}(\sigma_y - \sigma_z) \quad x = 3L_B, \quad \sigma_y \geq \sigma_z \quad (1-29a)$$

$$L_y = 0 \quad x = 3L_B, \quad \sigma_y < \sigma_z$$

L_B equals the minimum of h_b and h_w , where h_b is the building height and h_w the projected (crosswind) building width. A is a linear decay factor and is discussed in more detail in Section 1.1.5.3.2. If there is no enhancement of F_y or if the enhanced F_y is less than the enhanced F_z , the initial plume will be represented by a circle of radius R_o . The $\sqrt{2}$ factor converts the Gaussian F_z to an equivalent uniform circular distribution and $\sqrt{2\Pi}$ converts F_y to an equivalent uniform rectangular distribution. Both F_y and F_z are evaluated at $x = 3L_B$, and are taken as the larger of the building enhanced sigmas and the sigmas obtained from the curves (see Section 1.1.5.3). The value of F_z used in the calculation of L_y also includes the linear decay term, A .

The rise of a downwashed finite line source was solved in the BLP model (Scire and Schulman, 1980). The neutral distance-dependent rise (Z) is given by:

$$Z^3 + \left(\frac{3L_y}{\Pi\beta} + \frac{3R_o}{\beta} \right) Z^2 + \left(\frac{6R_oL_y}{\Pi\beta^2} + \frac{3R_o^2}{\beta^2} \right) Z = - \quad (1-30)$$

The stable distance-dependent rise is calculated by:

$$Z^3 + \left(\frac{3L_y}{\pi\beta} + \frac{3R_o}{\beta} \right) Z^2 + \left(\frac{6R_o L_y}{\pi\beta^2} + \frac{3R_o^2}{\beta^2} \right) Z = \frac{3F_b x}{2\beta^2 u} \quad (1-31a)$$

with a maximum stable buoyant rise given by:

$$Z^3 + \left(\frac{3L_y}{\pi\beta} + \frac{3R_o}{\beta} \right) Z^2 + \left(\frac{6R_o L_y}{\pi\beta^2} + \frac{3R_o^2}{\beta^2} \right) Z = \frac{6F_b}{\beta^2 u_s s} \quad (1-31b)$$

where:

F_b = buoyancy flux term (Equation 1-8) (m^4/s^3)

F_m = momentum flux term (Equation 1-9) (m^4/s^2)

x = downwind distance (m)

u_s = wind speed at release height (m/s)

v_s = stack exit velocity (m/s)

d_s = stack diameter (m)

S = entrainment coefficient (=0.6)

S_j = jet entrainment coefficient = $\frac{1}{3} + \frac{u_s}{v_s}$

s = stability parameter = $g \frac{\partial\theta/\partial z}{T_a}$

The larger of momentum and buoyant rise, determined separately by alternately setting F_b or $F_m = 0$ and solving for Z , is selected for plume height calculations for Schulman-Scire downwash. In the ISC models, Z is determined by solving the cubic equation using Newton's method.

1.1.5 The Dispersion Parameters

1.1.5.1 Point Source Dispersion Parameters.

Equations that approximately fit the Pasquill-Gifford curves (Turner, 1970) are used to calculate F_y and F_z (in meters) for the rural mode. The equations used to calculate F_y are of the form:

$$\sigma_y = 465.11628 (x) \tan(\text{TH}) \quad (1-32)$$

where:

$$\text{TH} = 0.017453293 [c - d \ln(x)] \quad (1-33)$$

In Equations (1-32) and (1-33) the downwind distance x is in kilometers, and the coefficients c and d are listed in Table 1-1. The equation used to calculate F_z is of the form:

$$\sigma_z = ax^b \quad (1-34)$$

where the downwind distance x is in kilometers and F_z is in meters. The coefficients a and b are given in Table 1-2.

Tables 1-3 and 1-4 show the equations used to determine F_y and F_z for the urban option. These expressions were determined by Briggs as reported by Gifford (1976) and represent a best fit to urban vertical diffusion data reported by McElroy and Pooler (1968). While the Briggs functions are assumed to be valid for downwind distances less than 100m, the user is cautioned that concentrations at receptors less than 100m from a source may be suspect.

TABLE 1-1

PARAMETERS USED TO CALCULATE PASQUILL-GIFFORD F_y

$$F_y = 465.11628 (x) \tan(\text{TH})$$

$$\text{TH} = 0.017453293 [c - d \ln(x)]$$

Pasquill Stability Category	c	d
A	24.1670	2.5334
B	18.3330	1.8096
C	12.5000	1.0857
D	8.3330	0.72382
E	6.2500	0.54287
F	4.1667	0.36191

where F_y is in meters and x is in kilometers

TABLE 1-2
PARAMETERS USED TO CALCULATE PASQUILL-GIFFORD F_z

Pasquill Stability Category	x (km)	$F_z(\text{meters}) = ax^b$ (x in km)	
		a	b
A*	<.10	122.800	0.94470
	0.10 - 0.15	158.080	1.05420
	0.16 - 0.20	170.220	1.09320
	0.21 - 0.25	179.520	1.12620
	0.26 - 0.30	217.410	1.26440
	0.31 - 0.40	258.890	1.40940
	0.41 - 0.50	346.750	1.72830
	0.51 - 3.11	453.850	2.11660
	>3.11	**	**
B*	<.20	90.673	0.93198
	0.21 - 0.40	98.483	0.98332
	>0.40	109.300	1.09710
C*	All	61.141	0.91465
D	<.30	34.459	0.86974
	0.31 - 1.00	32.093	0.81066
	1.01 - 3.00	32.093	0.64403
	3.01 - 10.00	33.504	0.60486
	10.01 - 30.00	36.650	0.56589
	>30.00	44.053	0.51179

* If the calculated value of F_z exceed 5000 m, F_z is set to 5000 m.

** F_z is equal to 5000 m.

TABLE 1-2
(CONTINUED)

PARAMETERS USED TO CALCULATE PASQUILL-GIFFORD F_z

Pasquill Stability Category	x (km)	$F_z(\text{meters}) = ax^b$ (x in km)	
		a	b
E	<.10	24.260	0.83660
	0.10 - 0.30	23.331	0.81956
	0.31 - 1.00	21.628	0.75660
	1.01 - 2.00	21.628	0.63077
	2.01 - 4.00	22.534	0.57154
	4.01 - 10.00	24.703	0.50527
	10.01 - 20.00	26.970	0.46713
	20.01 - 40.00	35.420	0.37615
	>40.00	47.618	0.29592
F	<.20	15.209	0.81558
	0.21 - 0.70	14.457	0.78407
	0.71 - 1.00	13.953	0.68465
	1.01 - 2.00	13.953	0.63227
	2.01 - 3.00	14.823	0.54503
	3.01 - 7.00	16.187	0.46490
	7.01 - 15.00	17.836	0.41507
	15.01 - 30.00	22.651	0.32681
	30.01 - 60.00	27.074	0.27436
>60.00	34.219	0.21716	

TABLE 1-3

BRIGGS FORMULAS USED TO CALCULATE McELROY-POOLER F_y

Pasquill Stability Category	F_y (meters)*
A	$0.32 \times (1.0 + 0.0004 \times)^{-1/2}$
B	$0.32 \times (1.0 + 0.0004 \times)^{-1/2}$
C	$0.22 \times (1.0 + 0.0004 \times)^{-1/2}$
D	$0.16 \times (1.0 + 0.0004 \times)^{-1/2}$
E	$0.11 \times (1.0 + 0.0004 \times)^{-1/2}$
F	$0.11 \times (1.0 + 0.0004 \times)^{-1/2}$

* Where x is in meters

TABLE 1-4

BRIGGS FORMULAS USED TO CALCULATE McELROY-POOLER F_z

Pasquill Stability Category	F_z (meters)*
A	$0.24 \times (1.0 + 0.001 \times)^{1/2}$
B	$0.24 \times (1.0 + 0.001 \times)^{1/2}$
C	$0.20 \times$
D	$0.14 \times (1.0 + 0.0003 \times)^{-1/2}$
E	$0.08 \times (1.0 + 0.0015 \times)^{-1/2}$
F	$0.08 \times (1.0 + 0.0015 \times)^{-1/2}$

* Where x is in meters.

1.1.5.2 Lateral and Vertical Virtual Distances.

The equations in Tables 1-1 through 1-4 define the dispersion parameters for an ideal point source. However, volume sources have initial lateral and vertical dimensions. Also, as discussed below, building wake effects can enhance the initial growth of stack plumes. In these cases, lateral (x_y) and vertical (x_z) virtual distances are added by the ISC models to the actual downwind distance x for the F_y and F_z calculations. The lateral virtual distance in kilometers for the rural mode is given by:

$$x_y = \left(\frac{\sigma_{y0}}{p} \right)^{1/q} \quad (1-35)$$

where the stability-dependent coefficients p and q are given in Table 1-5 and F_{y0} is the standard deviation in meters of the lateral concentration distribution at the source. Similarly, the vertical virtual distance in kilometers for the rural mode is given by:

$$x_z = \left(\frac{\sigma_{z0}}{a} \right)^{1/b} \quad (1-36)$$

where the coefficients a and b are obtained from Table 1-2 and F_{z0} is the standard deviation in meters of the vertical concentration distribution at the source. It is important to note that the ISC model programs check to ensure that the x_z used to calculate F_z at $(x + x_z)$ in the rural mode is the x_z calculated using the coefficients a and b that correspond to the distance category specified by the quantity $(x + x_z)$.

To determine virtual distances for the urban mode, the functions displayed in Tables 1-3 and 1-4 are solved for x . The solutions are quadratic formulas for the lateral virtual

distances; and for vertical virtual distances the solutions are cubic equations for stability classes A and B, a linear equation for stability class C, and quadratic equations for stability classes D, E, and F. The cubic equations are solved by iteration using Newton's method.

TABLE 1-5
 COEFFICIENTS USED TO CALCULATE LATERAL VIRTUAL DISTANCES
 FOR PASQUILL-GIFFORD DISPERSION RATES

Pasquill Stability Category	p	q
A	209.14	0.890
B	154.46	0.902
C	103.26	0.917
D	68.26	0.919
E	51.06	0.921
F	33.92	0.919

$$x_y = \left(\frac{\sigma_{yn}}{p} \right)^{1/q}$$

1.1.5.3 Procedures Used to Account for the Effects of Building Wakes on Effluent Dispersion.

The procedures used by the ISC models to account for the effects of the aerodynamic wakes and eddies produced by plant buildings and structures on plume dispersion originally followed the suggestions of Huber (1977) and Snyder (1976). Their suggestions are principally based on the results of wind-tunnel experiments using a model building with a crosswind dimension double that of the building height. The atmospheric turbulence simulated in the wind-tunnel experiments was

intermediate between the turbulence intensity associated with the slightly unstable Pasquill C category and the turbulence intensity associated with the neutral D category. Thus, the data reported by Huber and Snyder reflect a specific stability, building shape and building orientation with respect to the mean wind direction. It follows that the ISC wake-effects evaluation procedures may not be strictly applicable to all situations. The ISC models also provide for the revised treatment of building wake effects for certain sources, which uses modified plume rise algorithms, following the suggestions of Schulman and Hanna (1986). This treatment is largely based on the work of Scire and Schulman (1980). When the stack height is less than the building height plus half the lesser of the building height or width, the methods of Schulman and Scire are followed. Otherwise, the methods of Huber and Snyder are followed. In the ISC models, direction-specific building dimensions may be used with either the Huber-Snyder or Schulman-Scire downwash algorithms.

The wake-effects evaluation procedures may be applied by the user to any stack on or adjacent to a building. For regulatory application, a building is considered sufficiently close to a stack to cause wake effects when the distance between the stack and the nearest part of the building is less than or equal to five times the lesser of the height or the projected width of the building. For downwash analyses with direction-specific building dimensions, wake effects are assumed to occur if the stack is within a rectangle composed of two lines perpendicular to the wind direction, one at $5L_b$ downwind of the building and the other at $2L_b$ upwind of the building, and by two lines parallel to the wind direction, each at $0.5L_b$ away from each side of the building, as shown below:

```

Wind direction )))))))>
+))))) , ))
*
*          +)), ) ) ) ) ) ) ) ) ) ) * ))      1/2 Lb
*          +))- .)),
*          *Building*
*          *
*          .))))) , *
*          * *
*          .))- ) ) ) ) ) ) ) ) ) ) * ))      1/2 Lb
*          .))))) - ))
* <)) 2Lb)>*          * <)) 5Lb)>*

```

L_b is the lesser of the height and projected width of the building for the particular direction sector. For additional guidance on determining whether a more complex building configuration is likely to cause wake effects, the reader is referred to the Guideline for Determination of Good Engineering Practice Stack Height (Technical Support Document for the Stack Height Regulations) - Revised (EPA, 1985). In the following sections, the Huber and Snyder building downwash method is described followed by a description of the Schulman and Scire building downwash method.

1.1.5.3.1 Huber and Snyder building downwash procedures.

The first step in the wake-effects evaluation procedures used by the ISC model programs is to calculate the gradual plume rise due to momentum alone at a distance of two building heights using Equation (1-23) or Equation (1-25). If the plume height, h_e , given by the sum of the stack height (with no stack-tip downwash adjustment) and the momentum rise is greater than either 2.5 building heights ($2.5 h_b$) or the sum of the

building height and 1.5 times the building width ($h_b + 1.5 h_w$), the plume is assumed to be unaffected by the building wake. Otherwise the plume is assumed to be affected by the building wake.

The ISC model programs account for the effects of building wakes by modifying both F_y and F_z for plumes with plume height to building height ratios less than or equal to 1.2 and by modifying only F_z for plumes from stacks with plume height to building height ratios greater than 1.2 (but less than 2.5). The plume height used in the plume height to stack height ratios is the same plume height used to determine if the plume is affected by the building wake. The ISC models define buildings as squat ($h_w \geq h_b$) or tall ($h_w < h_b$). The ISC models include a general procedure for modifying F_z and F_y at distances greater than or equal to $3h_b$ for squat buildings or $3h_w$ for tall buildings. The air flow in the building cavity region is both highly turbulent and generally recirculating. The ISC models are not appropriate for estimating concentrations within such regions. The ISC assumption that this recirculating cavity region extends to a downwind distance of $3h_b$ for a squat building or $3h_w$ for a tall building is most appropriate for a building whose width is not much greater than its height. The ISC user is cautioned that, for other types of buildings, receptors located at downwind distances of $3h_b$ (squat buildings) or $3h_w$ (tall buildings) may be within the recirculating region.

The modified F_z equation for a squat building is given by:

$$\sigma_z' = 0.7h_b + 0.067(x-3h_b) \quad \text{for } 3h_b \leq x < 10h_b$$

or

(1-37)

$$= \sigma_z\{x + x_z\} \quad \text{for } x \geq 10h_b$$

where the building height h_b is in meters. For a tall building, Huber (1977) suggests that the width scale h_w replace h_b in Equation (1-37). The modified F_z equation for a tall building is then given by:

$$\sigma_z' = 0.7h_w + 0.067(x-3h_w) \quad \text{for } 3h_w \leq x < 10h_w$$

or

(1-38)

$$= \sigma_z\{x + x_z\} \quad \text{for } x \geq 10h_w$$

where h_w is in meters. It is important to note that F_z' is not permitted to be less than the point source value given in Tables 1-2 or 1-4, a condition that may occur.

The vertical virtual distance, x_z , is added to the actual downwind distance x at downwind distances beyond $10h_b$ for squat buildings or beyond $10h_w$ for tall buildings, in order to account for the enhanced initial plume growth caused by the building wake. The virtual distance is calculated from solutions to the equations for rural or urban sigmas provided earlier.

As an example for the rural options, Equations (1-34) and (1-37) can be combined to derive the vertical virtual distance x_z for a squat building. First, it follows from Equation (1-37) that the enhanced F_z is equal to $1.2h_b$ at a downwind distance of $10h_b$ in meters or $0.01h_b$ in kilometers. Thus, x_z

for a squat building is obtained from Equation (1-34) as follows:

$$\sigma_z \{0.01h_b\} = 1.2h_b = a(0.01h_b + x_z)^b \quad (1-39)$$

$$x_z = \left(\frac{1.2h_b}{a} \right)^{1/b} - 0.01h_b \quad (1-40)$$

where the stability-dependent constants a and b are given in Table 1-2. Similarly, the vertical virtual distance for tall buildings is given by:

$$x_z = \left(\frac{1.2h_v}{a} \right)^{1/b} - 0.01h_v \quad (1-41)$$

For the urban option, x_z is calculated from solutions to the equations in Table 1-4 for $F_z = 1.2h_b$ or $F_z = 1.2 h_w$ for tall or squat buildings, respectively.

For a squat building with a building width to building height ratio (h_w/h_b) less than or equal to 5, the modified F_y equation is given by:

$$\sigma_y' = 0.35h_v + 0.067(x - 3h_b) \quad \text{for } 3h_b \leq x < 10h_b \quad (1-42)$$

$$= \sigma_y \{x + x_y\} \quad \text{for } x \geq 10h_b$$

The lateral virtual distance is then calculated for this value of F_y .

For a building that is much wider than it is tall (h_w/h_b greater than 5), the presently available data are insufficient

to provide general equations for F_y . For a stack located toward the center of such a building (i.e., away from either end), only the height scale is considered to be significant. The modified F_y equation for a very squat building is then given by:

$$\begin{aligned}\sigma_y' &= 0.35h_b + 0.067(x-3h_b) && \text{for } 3h_b \leq x < 10h_b \\ &= \sigma_y\{x + x_y\} && \text{for } x \geq 10h_b\end{aligned}\tag{1-43}$$

For h_w/h_b greater than 5, and a stack located laterally within about 2.5 h_b of the end of the building, lateral plume spread is affected by the flow around the end of the building. With end effects, the enhancement in the initial lateral spread is assumed not to exceed that given by Equation (1-42) with h_w replaced by 5 h_b . The modified F_y equation is given by:

$$\begin{aligned}\sigma_y' &= 1.75h_b + 0.067(x-3h_b) && \text{for } 3h_b \leq x < 10h_b \\ &= \sigma_y\{x + x_y\} && \text{for } x \geq 10h_b\end{aligned}\tag{1-44}$$

The upper and lower bounds of the concentrations that can be expected to occur near a building are determined respectively using Equations (1-43) and (1-44). The user must specify whether Equation (1-43) or Equation (1-44) is to be used in the model calculations. In the absence of user instructions, the ISC models use Equation (1-43) if the building width to building height ratio h_w/h_b exceeds 5.

Although Equation (1-43) provides the highest concentration estimates for squat buildings with building width to building height ratios (h_w/h_b) greater than 5, the equation is applicable only to a stack located near the center of the building when the wind direction is perpendicular to the long side of the building (i.e., when the air flow over the portion of the building containing the source is two dimensional). Thus, Equation (1-44) generally is more appropriate than Equation (1-43). It is believed that Equations (1-43) and (1-44) provide reasonable limits on the extent of the lateral enhancement of dispersion and that these equations are adequate until additional data are available to evaluate the flow near very wide buildings.

The modified F_y equation for a tall building is given by:

$$\begin{aligned} \sigma_y' &= 0.35h_v + 0.067(x-3h_v) && \text{for } 3h_v \leq x < 10h_v \\ &= \sigma_y\{x + x_y\} && \text{for } x \geq 10h_v \end{aligned} \tag{1-45}$$

The ISC models print a message and do not calculate concentrations for any source-receptor combination where the source-receptor separation is less than 1 meter, and also for distances less than $3 h_b$ for a squat building or $3 h_w$ for a tall building under building wake effects. It should be noted that, for certain combinations of stability and building height and/or width, the vertical and/or lateral plume dimensions indicated for a point source by the dispersion curves at a downwind distance of ten building heights or widths can exceed the values given by Equation (1-37) or (1-38) and by Equation

(1-42) or (1-43). Consequently, the ISC models do not permit the virtual distances x_y and x_z to be less than zero.

1.1.5.3.2 Schulman and Scire refined building downwash procedures.

The procedures for treating building wake effects include the use of the Schulman and Scire downwash method. The building wake procedures only use the Schulman and Scire method when the physical stack height is less than $h_b + 0.5 L_B$, where h_b is the building height and L_B is the lesser of the building height or width. In regulatory applications, the maximum projected width is used. The features of the Schulman and Scire method are: (1) reduced plume rise due to initial plume dilution, (2) enhanced vertical plume spread as a linear function of the effective plume height, and (3) specification of building dimensions as a function of wind direction. The reduced plume rise equations were previously described in Section 1.1.4.11.

When the Schulman and Scire method is used, the ISC dispersion models specify a linear decay factor, to be included in the F_z 's calculated using Equations (1-37) and (1-38), as follows:

$$\sigma_z'' = A\sigma_z' \quad (1-46)$$

where F_z' is from either Equation (1-37) or (1-38) and A is the linear decay factor determined as follows:

$$\begin{aligned} A &= 1 && \text{if } h_e \leq h_b \\ A &= \frac{h_b - h_e}{2L_B} + 1 && \text{if } h_b < h_e \leq h_b + 2L_B \\ A &= 0 && \text{if } h_e > h_b + 2L_B \end{aligned} \quad (1-47)$$

where the plume height, h_e , is the height due to gradual momentum rise at $2 h_b$ used to check for wake effects. The effect of the linear decay factor is illustrated in Figure 1-1. For Schulman-Scire downwash cases, the linear decay term is also used in calculating the vertical virtual distances with Equations (1-40) to (1-41).

When the Schulman and Scire building downwash method is used the ISC models require direction specific building heights and projected widths for the downwash calculations. The ISC models also accept direction specific building dimensions for Huber-Snyder downwash cases. The user inputs the building height and projected widths of the building tier associated with the greatest height of wake effects for each ten degrees of wind direction. These building heights and projected widths are the same as are used for GEP stack height calculations. The user is referred to EPA (1986) for calculating the appropriate building heights and projected widths for each direction. Figure 1-2 shows an example of a two tiered building with different tiers controlling the height that is appropriate for use for different wind directions. For an east or west wind the lower tier defines the appropriate height and width, while for a north or south wind the upper tier defines the appropriate values for height and width.

1.1.5.4 Procedures Used to Account for Buoyancy-Induced Dispersion.

The method of Pasquill (1976) is used to account for the initial dispersion of plumes caused by turbulent motion of the plume and turbulent entrainment of ambient air. With this

method, the effective vertical dispersion F_{ze} is calculated as follows:

$$\sigma_{ze} = \left[\sigma_z^2 + \left(\frac{\Delta h}{3.5} \right)^2 \right]^{1/2} \quad (1-48)$$

where F_z is the vertical dispersion due to ambient turbulence and Δh is the plume rise due to momentum and/or buoyancy. The lateral plume spread is parameterized using a similar expression:

$$\sigma_{ye} = \left[\sigma_y^2 + \left(\frac{\Delta h}{3.5} \right)^2 \right]^{1/2} \quad (1-49)$$

where F_y is the lateral dispersion due to ambient turbulence. It should be noted that Δh is the distance-dependent plume rise if the receptor is located between the source and the distance to final rise, and final plume rise if the receptor is located beyond the distance to final rise. Thus, if the user elects to use final plume rise at all receptors the distance-dependent plume rise is used in the calculation of buoyancy-induced dispersion and the final plume rise is used in the concentration equations. It should also be noted that buoyancy-induced dispersion is not used when the Schulman-Scire downwash option is in effect.

1.1.6 The Vertical Term

The Vertical Term (V), which is included in Equation (1-1), accounts for the vertical distribution of the Gaussian plume. It includes the effects of source elevation, receptor elevation, plume rise (Section 1.1.4), limited mixing in the vertical, and the gravitational settling and dry deposition of particulates. In addition to the plume height, receptor height and mixing height, the computation of the Vertical Term requires the vertical dispersion parameter (F_z) described in Section 1.1.5.

1.1.6.1 The Vertical Term Without Dry Deposition.

In general, the effects on ambient concentrations of gravitational settling and dry deposition can be neglected for gaseous pollutants and small particulates (less than about 0.1 microns in diameter). The Vertical Term without deposition effects is then given by:

$$\begin{aligned}
 V = & \exp \left[-0.5 \left(\frac{z_r - h_e}{\sigma_z} \right)^2 \right] + \exp \left[-0.5 \left(\frac{z_r + h_e}{\sigma_z} \right)^2 \right] \\
 & + \sum_{i=1} \left\{ \exp \left[-0.5 \left(\frac{H_1}{\sigma_z} \right)^2 \right] + \exp \left[-0.5 \left(\frac{H_2}{\sigma_z} \right)^2 \right] \right. \\
 & \left. + \exp \left[-0.5 \left(\frac{H_3}{\sigma_z} \right)^2 \right] + \exp \left[-0.5 \left(\frac{H_4}{\sigma_z} \right)^2 \right] \right\}
 \end{aligned} \tag{1-50}$$

where:

$$h_e = h_s +)h$$

$$H_1 = z_r - (2iz_i - h_e)$$

$$H_2 = z_r + (2iz_i - h_e)$$

$$H_3 = z_r - (2iz_i + h_e)$$

$$H_4 = z_r + (2iz_i + h_e)$$

z_r = receptor height above ground (flagpole) (m)

z_i = mixing height (m)

The infinite series term in Equation (1-50) accounts for the effects of the restriction on vertical plume growth at the top of the mixing layer. As shown by Figure 1-3, the method of image sources is used to account for multiple reflections of the plume from the ground surface and at the top of the mixed layer. It should be noted that, if the effective stack height, h_e , exceeds the mixing height, z_i , the plume is assumed to fully penetrate the elevated inversion and the ground-level concentration is set equal to zero.

Equation (1-50) assumes that the mixing height in rural and urban areas is known for all stability categories. As explained below, the meteorological preprocessor program uses mixing heights derived from twice-daily mixing heights calculated using the Holzworth (1972) procedures. The ISC models currently assume unlimited vertical mixing under stable conditions, and therefore delete the infinite series term in Equation (1-50) for the E and F stability categories.

The Vertical Term defined by Equation (1-50) changes the form of the vertical concentration distribution from Gaussian to rectangular (i.e., a uniform concentration within the surface mixing layer) at long downwind distances. Consequently, in order to reduce computational time without a loss of accuracy, Equation (1-50) is changed to the form:

$$v = \frac{\sqrt{2\pi}\sigma_z}{z_i} \quad (1-51)$$

at downwind distances where the F_z/z_i ratio is greater than or equal to 1.6.

The meteorological preprocessor program, RAMMET, used by the ISC Short Term model uses an interpolation scheme to assign hourly rural and urban mixing heights on the basis of the early morning and afternoon mixing heights calculated using the Holzworth (1972) procedures. The procedures used to interpolate hourly mixing heights in urban and rural areas are illustrated in Figure 1-4, where:

$H_m\{\max\}$ = maximum mixing height on a given day

$H_m\{\min\}$ = minimum mixing height on a given day

MN = midnight

SR = sunrise

SS = sunset

The interpolation procedures are functions of the stability category for the hour before sunrise. If the hour before sunrise is neutral, the mixing heights that apply are indicated by the dashed lines labeled neutral in Figure 1-4. If the hour before sunrise is stable, the mixing heights that apply are indicated by the dashed lines labeled stable. It should be pointed out that there is a discontinuity in the rural mixing height at sunrise if the preceding hour is stable. As explained above, because of uncertainties about the applicability of Holzworth mixing heights during periods of E and F stability, the ISC models ignore the interpolated mixing heights for E and F stability, and treat such cases as having unlimited vertical mixing.

1.1.6.2 The Vertical Term in Elevated Simple Terrain.

The ISC models make the following assumption about plume behavior in elevated simple terrain (i.e., terrain that exceeds the stack base elevation but is below the release height):

- The plume axis remains at the plume stabilization height above mean sea level as it passes over elevated or depressed terrain.
- The mixing height is terrain following.
- The wind speed is a function of height above the surface (see Equation (1-6)).

Thus, a modified plume stabilization height h_e' is substituted for the effective stack height h_e in the Vertical Term given by Equation (1-50). For example, the effective plume stabilization height at the point x, y is given by:

$$h_e' = h_e + z_s - z|_{(x,y)} \quad (1-52)$$

where:

- z_s = height above mean sea level of the base of the stack (m)
- $z^*_{(x,y)}$ = height above mean sea level of terrain at the receptor location (x,y) (m)

It should also be noted that, as recommended by EPA, the ISC models "truncate" terrain at stack height as follows: if the terrain height $z - z_s$ exceeds the source release height, h_s , the elevation of the receptor is automatically "chopped off" at the physical release height. The user is cautioned that concentrations at these complex terrain receptors are subject to considerable uncertainty. Figure 1-5 illustrates the terrain-adjustment procedures used by the ISC models for simple

elevated terrain. The vertical term used with the complex terrain algorithms in ISC is described in Section 1.5.6.

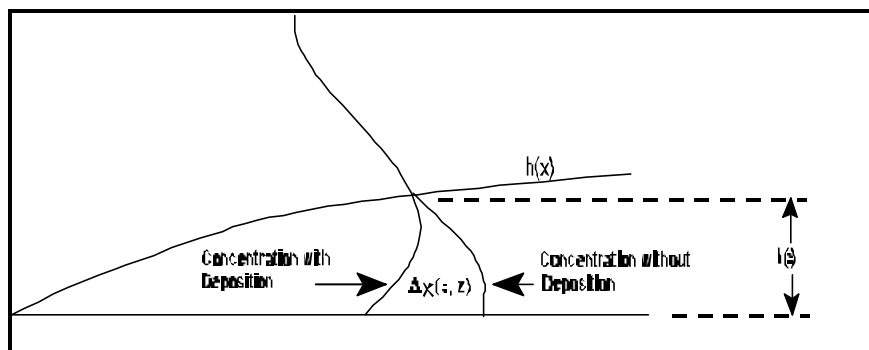
1.1.6.3 The Vertical Term With Dry Deposition.

Particulates are brought to the surface through the combined processes of turbulent diffusion and gravitational settling. Once near the surface, they may be removed from the atmosphere and deposited on the surface. This removal is modeled in terms of a deposition velocity (v_d) and the gravitational velocity (v_g), which are described in Section 1.3.1, by assuming that the deposition flux of material to the surface is equal to the product $P_d(v_d + v_g)$, where P_d is the airborne concentration at the surface. As the plume of airborne particulates is transported downwind, such deposition near the surface reduces the concentration of particulates in the plume, and thereby alters the vertical distribution of the remaining particulates. Furthermore, the particles will also move steadily nearer to the surface at a rate equal to their gravitational settling velocity (v_g). As a result, the plume centerline height is reduced.

A dry deposition and settling algorithm developed by Venkatram (1998) is used to calculate the dry deposition flux at the surface. In this algorithm, the deposition and the gravitation settling are treated as independent sequential processes, both of which cause the removal of plume mass at the surface. The removal due to the deposition process is accounted for by calculating a "depleted vertical term," while the gravitational settling is accounted for by simulating a slumping plume. Both of these processes are discussed below.

Dry Deposition

We
 can
 constru
 ct an
 approxi
 mate
 model



for dispersion in the presence of dry deposition by assuming that the effects of dry deposition are confined to a distance $h(x)$ next to the ground, as shown below.

The effect of dry deposition appears through the difference in concentration, $\Delta P(x, z)$, between the concentration profiles with and without deposition. This difference goes to zero at $z = h(x)$. To specify the shape of the difference profile, $\Delta P(x, z)$, we write the diffusion equation for the two profiles:

$$u_s \left(\frac{\partial \chi}{\partial x} \right) = \frac{\partial}{\partial z} \left(K \frac{\partial \chi}{\partial z} \right) \tag{1-53a}$$

and

$$u_s \left(\frac{\partial \chi_d}{\partial x} \right) = \frac{\partial}{\partial z} \left(K \frac{\partial \chi_d}{\partial z} \right) \quad (1-53b)$$

where $P(x, z)$ refers to the concentration profile without deposition, and $P_d(x, z)$ refers to that with deposition. If we subtract Equation (1-53b) from Equation (1-53a), we obtain the equation for the concentration difference profile,

$$u_s \left(\frac{\partial \Delta \chi}{\partial x} \right) = \frac{\partial}{\partial z} \left(K \frac{\partial \Delta \chi}{\partial z} \right) \quad (1-54)$$

Now, we integrate this equation between $z=0$ and $z=h(x)$ to obtain:

$$u_s \frac{\partial}{\partial x} \int_0^{h(x)} \Delta \chi(x, z) dz = K \left(\frac{\partial \Delta \chi}{\partial z} \right)_{z=h(x)} - K \left(\frac{\partial \Delta \chi}{\partial z} \right)_{z=0} \quad (1-55)$$

The second term on the right hand side of the Equation (1-55) can be evaluated by noticing that the vertical flux at the ground is equal to that removed by dry deposition,

$$-K \frac{\partial (\chi - \chi_d)}{\partial z} = K \frac{\partial \chi_d}{\partial z} = v_d \chi_d \text{ at } z=0 \quad (1-56)$$

Because

$$\chi_d(x, 0) = \chi(x, 0) - \Delta \chi(x, 0) \quad (1-57a)$$

we can rewrite equation (1-56) as

$$-K \frac{\partial (\chi - \chi_d)}{\partial z} = v_d (\chi(x, 0) - \Delta \chi(x, 0)) \quad (1-57b)$$

We can always define $h(x)$ so that the gradient of the concentration difference profile is zero at $z=h(x)$; then, the first term on the right hand side of Equation (1-55) disappears. A concentration difference profile that meets the zero gradient assumption at $z=h(x)$ is

$$\Delta \chi(x, z) = \Delta \chi(x, 0) \left(1 - \frac{z}{h(x)} \right)^2 \quad (1-58)$$

If we substitute Equation (1-58) into Equation (1-55) and integrate, we find

$$\frac{d}{dx} \left(\frac{h(x)}{3} \Delta \chi(x, 0) \right) = \frac{v_d}{u_s} (\chi(x, 0) - \Delta \chi(x, 0)) \quad (1-59)$$

Integrating Equation (1-59) yields,

$$\begin{aligned} n(x+\Delta x) = n(x) e^{-\bar{\alpha} \Delta x} + m(x+\Delta x) \left[1 - \frac{m(x)}{m(x+\Delta x)} e^{-\bar{\alpha} \Delta x} \right] \\ - \frac{\Delta x}{2} \left[m(x+\Delta x) \alpha(x+\Delta x) + m(x) \alpha(x) e^{-\bar{\alpha} \Delta x} \right] \end{aligned} \quad (1-60)$$

where:

$$\begin{aligned}
 n(x) &= \chi_d(x, 0) h(x) / 3 \\
 m(x) &= \chi(x, 0) h(x) / 3 \\
 \chi_d(x, 0) &= \text{surface concentration with deposition} \\
 \chi(x, 0) &= \text{surface concentration without deposition} \\
 \alpha(x) &= \left(\frac{3v_d}{h(x) u_s} \right) \\
 \bar{\alpha} &= \left(\frac{\alpha(x+\Delta x) + \alpha(x)}{2} \right) \\
 \Delta x &= \text{interval of integration}
 \end{aligned}$$

All else being equal, Equation (1-60) can be re-written by replacing the concentrations (P and P_d) with the corresponding vertical terms (V and V_d) as follows:

$$\begin{aligned}
 n(x+\Delta x) &= n(x) e^{-\bar{\alpha}\Delta x} + m(x+\Delta x) \left[1 - \frac{m(x)}{m(x+\Delta x)} e^{-\bar{\alpha}\Delta x} \right] \\
 &\quad - \frac{\Delta x}{2} [m(x+\Delta x) \alpha(x+\Delta x) + m(x) \alpha(x) e^{-\bar{\alpha}\Delta x}]
 \end{aligned} \tag{1-61}$$

where:

$$\begin{aligned}
 n(x) &= V_d(x, 0) h(x) / 3 \\
 m(x) &= V(x, 0) h(x) / 3 \\
 V_d(x, 0) &= \text{depleted vertical term at surface} \\
 V(x, 0) &= \text{un-depleted vertical term at surface}
 \end{aligned}$$

From the solution of Equation (1-61), V_d can be calculated as follows:

$$V_d(x, 0) = \frac{n(x)}{(h(x) / 3)} \tag{1-61a}$$

Equation (1-61) can be easily implemented if $h(x)$ is known. As a starting point, it is reasonable to choose

$$h(x) = \beta \sigma_z \quad (1-62)$$

where $\beta = 2.0$ is an empirically determined constant.

Because particle settling is treated in a separate step, described below, it should be noted that the dry deposition velocity used in the above calculations does not include the particle settling velocity.

Particle Settling

One of the simplest ways of accounting for particle settling is to assume that the whole plume slumps towards the ground, but the concentration of plume elements remains unchanged. This means that the concentration at any height, z , is equal to that at $(z + xv_g/u_s)$, where " xv_g/u_s " is the distance by which the plume has settled. This also implies that plume material, over a distance " xv_g/u_s " next to the ground, will be removed. While this concept is seemingly crude, it is consistent with the assumption that settling can be represented as an advective term, $v_g(MP/Mz)$, in the mass conservation equation.

In many applications, the removal of material from the plume may be extremely small. When this happens, the vertical term is virtually unchanged ($V_d = V$). The deposition flux can then be approximated as $P(v_d + v_g)$ rather than $P_d(v_d + v_g)$. The plume depletion calculations are optional, so that the added

expense of computing P_d can be avoided. Not considering the effects of dry depletion results in conservative estimates of both concentration and deposition, since material deposited on the surface is not removed from the plume.

1.1.7 The Decay Term (D)

The Decay Term in Equation (1-1) is a simple method of accounting for pollutant removal by physical or chemical processes. It is of the form:

$$D = \exp\left(-\psi \frac{x}{u_s}\right) \quad \text{for } \psi > 0$$
(1-63)

$$= 1 \quad \text{for } \psi = 0$$

where:

R = the decay coefficient (s^{-1}) (a value of zero means decay is not considered)

x = downwind distance (m)

For example, if $T_{1/2}$ is the pollutant half life in seconds, the user can obtain R from the relationship:

$$\psi = \frac{0.693}{T_{1/2}}$$
(1-64)

The default value for R is zero. That is, decay is not considered in the model calculations unless R is specified.

However, a decay half life of 4 hours ($R = 0.0000481 \text{ s}^{-1}$) is automatically assigned for SO_2 when modeled in the urban mode.

1.2 NON-POINT SOURCE EMISSIONS

1.2.1 General

The ISC models include algorithms to model volume, area and open-pit sources, in addition to point sources. These non-point source options of the ISC models are used to simulate the effects of emissions from a wide variety of industrial sources. In general, the ISC volume source model is used to simulate the effects of emissions from sources such as building roof monitors and line sources (for example, conveyor belts and rail lines). The ISC area source model is used to simulate the effects of fugitive emissions from sources such as storage piles and slag dumps. The ISC open pit source model is used to simulate fugitive emissions from below-grade open pits, such as surface coal mines or stone quarries.

1.2.2 The Short-Term Volume Source Model

The ISC models use a virtual point source algorithm to model the effects of volume sources, which means that an imaginary or virtual point source is located at a certain distance upwind of the volume source (called the virtual distance) to account for the initial size of the volume source plume. Therefore, Equation (1-1) is also used to calculate concentrations produced by volume source emissions.

There are two types of volume sources: surface-based sources, which may also be modeled as area sources, and elevated sources. An example of a surface-based source is a surface rail line. The effective emission height h_e for a surface-based source is usually set equal to zero. An example of an elevated source is an elevated rail line with an effective emission height h_e set equal to the height of the rail line. If the volume source is elevated, the user assigns the effective emission height h_e , i.e., there is no plume rise associated with volume sources. The user also assigns initial lateral (F_{y0}) and vertical (F_{z0}) dimensions for the volume source. Lateral (x_y) and vertical (x_z) virtual distances are added to the actual downwind distance x for the F_y and F_z calculations. The virtual distances are calculated from solutions to the sigma equations as is done for point sources with building downwash.

The volume source model is used to simulate the effects of emissions from sources such as building roof monitors and for line sources (for example, conveyor belts and rail lines). The north-south and east-west dimensions of each volume source used in the model must be the same. Table 1-6 summarizes the general procedures suggested for estimating initial lateral (F_{y0}) and vertical (F_{z0}) dimensions for single volume sources and for multiple volume sources used to represent a line source. In the case of a long and narrow line source such as a rail line, it may not be practical to divide the source into N volume sources, where N is given by the length of the line source divided by its width. The user can obtain an approximate representation of the line source by placing a smaller number of volume sources at equal intervals along the line source, as shown in Figure 1-8. In general, the spacing

between individual volume sources should not be greater than twice the width of the line source. However, a larger spacing can be used if the ratio of the minimum source-receptor separation and the spacing between individual volume sources is greater than about 3. In these cases, concentrations calculated using fewer than N volume sources to represent the line source converge to the concentrations calculated using N volume sources to represent the line source as long as sufficient volume sources are used to preserve the horizontal geometry of the line source.

Figure 1-8 illustrates representations of a curved line source by multiple volume sources. Emissions from a line source or narrow volume source represented by multiple volume sources are divided equally among the individual sources unless there is a known spatial variation in emissions. Setting the initial lateral dimension F_{y_0} equal to $W/2.15$ in Figure 1-8(a) or $2W/2.15$ in Figure 1-8(b) results in overlapping Gaussian distributions for the individual sources. If the wind direction is normal to a straight line source that is represented by multiple volume sources, the initial crosswind concentration distribution is uniform except at the edges of the line source. The doubling of F_{y_0} by the user in the approximate line-source representation in Figure 1-8(b) is offset by the fact that the emission rates for the individual volume sources are also doubled by the user.

TABLE 1-6

SUMMARY OF SUGGESTED PROCEDURES FOR ESTIMATING
INITIAL LATERAL DIMENSIONS F_{y0} AND
INITIAL VERTICAL DIMENSIONS F_{z0} FOR VOLUME AND LINE SOURCES

Type of Source	Procedure for Obtaining Initial Dimension
(a) Initial Lateral Dimensions (F_{y0})	
Single Volume Source	F_{y0} = length of side divided by 4.3
Line Source Represented by Adjacent Volume Sources (see Figure 1-8(a))	F_{y0} = length of side divided by 2.15
Line Source Represented by Separated Volume Sources (see Figure 1-8(b))	F_{y0} = center to center distance divided by 2.15
(b) Initial Vertical Dimensions (F_{z0})	
Surface-Based Source ($h_e = 0$)	F_{z0} = vertical dimension of source divided by 2.15
Elevated Source ($h_e > 0$) on or Adjacent to a Building	F_{z0} = building height divided by 2.15
Elevated Source ($h_e > 0$) not on or Adjacent to a Building	F_{z0} = vertical dimension of source divided by 4.3

1.2.3 The Short-Term Area Source Model

The ISC Short Term area source model is based on a numerical integration over the area in the upwind and crosswind directions of the Gaussian point source plume formula given in Equation (1-1). Individual area sources may be represented as rectangles with aspect ratios (length/width) of up to 10 to 1. In addition, the rectangles may be rotated relative to a north-south and east-west orientation. As shown by Figure 1-9, the effects of an irregularly shaped area can be simulated by dividing the area source into multiple areas. Note that the size and shape of the individual area sources in Figure 1-9 varies; the only requirement is that each area source must be a rectangle. As a result, an irregular area source can be represented by a smaller number of area sources than if each area had to be a square shape. Because of the flexibility in specifying elongated area sources with the Short Term model, up to an aspect ratio of about 10 to 1, the ISCST area source algorithm may also be useful for modeling certain types of line sources.

The ground-level concentration at a receptor located downwind of all or a portion of the source area is given by a double integral in the upwind (x) and crosswind (y) directions as:

$$C = \frac{Q_s K}{2\pi u_s} \int_x \frac{VD}{\sigma_y \sigma_z} \left(\int_y \exp \left[-0.5 \left(\frac{y}{\sigma_y} \right)^2 \right] dy \right) dx \quad (1-65)$$

where:

Q_A = area source emission rate (mass per unit area per unit time)

K = units scaling coefficient (Equation (1-1))

V = vertical term (see Section 1.1.6)

D = decay term as a function of x (see Section 1.1.7)

The Vertical Term is given by Equation (1-50) or Equation (1-54) with the effective emission height, h_e , being the physical release height assigned by the user. In general, h_e should be set equal to the physical height of the source of emissions above local terrain height. For example, the emission height h_e of a slag dump is the physical height of the slag dump.

Since the ISCST algorithm estimates the integral over the area upwind of the receptor location, receptors may be located within the area itself, downwind of the area, or adjacent to the area. However, since F_z goes to 0 as the downwind distance goes to 0 (see Section 1.1.5.1), the plume function is infinite for a downwind receptor distance of 0. To avoid this singularity in evaluating the plume function, the model arbitrarily sets the plume function to 0 when the receptor distance is less than 1 meter. As a result, the area source algorithm will not provide reliable results for receptors located within or adjacent to very small areas, with dimensions on the order of a few meters across. In these cases, the receptor should be placed at least 1 meter outside of the area.

In Equation (1-65), the integral in the lateral (i.e., crosswind or y) direction is solved analytically as follows:

$$\int_y \exp\left[-0.5\left(\frac{y}{\sigma_y}\right)^2\right] dy = \text{erfc}\left(\frac{y}{\sigma_y}\right) \quad (1-66)$$

where erfc is the complementary error function.

In Equation (1-65), the integral in the longitudinal (i.e., upwind or x) direction is approximated using numerical methods based on Press, et al (1986). Specifically, the ISCST model estimates the value of the integral, I, as a weighted average of previous estimates, using a scaled down extrapolation as follows:

$$I = \int_x \frac{VD}{\sigma_y \sigma_z} \text{erfc}\left(\frac{y}{\sigma_y}\right) dx = I_{2N} + \frac{(I_{2N} - I_N)}{3} \quad (1-67)$$

where the integral term refers to the integral of the plume function in the upwind direction, and I_N and I_{2N} refer to successive estimates of the integral using a trapezoidal approximation with N intervals and 2N intervals. The number of intervals is doubled on successive trapezoidal estimates of the integral. The ISCST model also performs a Romberg integration by treating the sequence I_k as a polynomial in k. The Romberg integration technique is described in detail in Section 4.3 of Press, et al (1986). The ISCST model uses a set of three criteria to determine whether the process of integrating in the upwind direction has "converged." The calculation process will be considered to have converged, and the most recent estimate of the integral used, if any of the following conditions is true:

- 1) if the number of "halving intervals" (N) in the trapezoidal approximation of the integral has reached 10, where the number of individual elements in the approximation is given by $1 + 2^{N-1} = 513$ for N of 10;
- 2) if the extrapolated estimate of the real integral (Romberg approximation) has converged to within a tolerance of 0.0001 (i.e., 0.01 percent), and at least 4 halving intervals have been completed; or
- 3) if the extrapolated estimate of the real integral is less than 1.0E-10, and at least 4 halving intervals have been completed.

The first condition essentially puts a time limit on the integration process, the second condition checks for the accuracy of the estimate of the integral, and the third condition places a lower threshold limit on the value of the integral. The result of these numerical methods is an estimate of the full integral that is essentially equivalent to, but much more efficient than, the method of estimating the integral as a series of line sources, such as the method used by the PAL 2.0 model (Petersen and Rumsey, 1987).

1.2.4 The Short-Term Open Pit Source Model

The ISC open pit source model is used to estimate impacts for particulate emissions originating from a below-grade open pit, such as a surface coal mine or a stone quarry. The ISC models allow the open pit source to be characterized by a rectangular shape with an aspect ratio (length/width) of up to 10 to 1. The rectangular pit may also be rotated relative to a north-south and east-west orientation. Since the open pit model does not apply to receptors located within the boundary of the pit, the concentration at those receptors will be set to zero by the ISC models.

The model accounts for partial retention of emissions within the pit by calculating an escape fraction for each particle size category. The variations in escape fractions across particle sizes result in a modified distribution of mass escaping from the pit. Fluid modeling has shown that within-pit emissions have a tendency to escape from the upwind side of the pit. The open pit algorithm simulates the escaping pit emissions by using an effective rectangular area source using the ISC area source algorithm described in Section 1.2.3. The shape, size and location of the effective area source varies with the wind direction and the relative depth of the pit. Because the shape and location of the effective area source varies with wind direction, a single open pit source should not be subdivided into multiple pit sources.

The escape fraction for each particle size category, g_i , is calculated as follows:

$$\varepsilon_i = \frac{1}{(1 + v_g / (\alpha U_r))} \quad (1-68)$$

where:

v_g = is the gravitational settling velocity (m/s),

U_r = is the approach wind speed at 10m (m/s),

" = is the proportionality constant in the relationship between flux from the pit and the product of U_r and concentration in the pit (Thompson, 1994).

The gravitational settling velocity, v_g , is computed as described in Section 1.3.2 for each particle size category. Thompson (1994) used laboratory measurements of pollutant residence times in a variety of pit shapes typical of actual mines and determined that a single value of " = 0.029 worked well for all pits studied.

The adjusted emission rate (Q_i) for each particle size category is then computed as:

$$Q_i = \varepsilon_i \cdot \phi_i \cdot Q \quad (1-69)$$

where Q is the total emission rate (for all particles) within the pit, N_i is the original mass fraction for the given size category, and g is the escape fraction calculated from Equation (1-68). The adjusted total emission rate (for all particles escaping the pit), Q_a , is the sum of the Q_i for all particle categories calculated from Equation 1-69. The mass

fractions (of particles escaping the pit), N_{ai} , for each category is:

$$\phi_{ai} = Q_i / Q_a \quad (1-70)$$

Because of particle settling within the pit, the distribution of mass escaping the pit is different than that emitted within the pit. The adjusted total particulate emission rate, Q_a , and the adjusted mass fractions, N_{ai} , reflect this change, and it is these adjusted values that are used for modeling the open pit emissions.

The following describes the specification of the location, dimensions and adjusted emissions for the effective area source used for modeling open pit emissions. Consider an arbitrary rectangular-shaped pit with an arbitrary wind direction as shown in Figure 1-10. The steps that the model uses for determining the effective area source are as follows:

1. Determine the upwind sides of the pit based on the wind direction.
2. Compute the along wind length of the pit (R) based on the wind direction and the pit geometry. R varies between the lengths of the two sides of the rectangular pit as follows:

$$R = L \cdot (1 - \theta/90) + W \cdot (\theta/90) \quad (1-71)$$

where L is the long axis and W is the short axis of the pit, and θ is the wind direction relative to the long axis (L) of the pit (therefore θ varies between 0° and 90°). Note that with this formulation and a

square pit, the value of R will remain constant with wind direction at $R = L = W$. The along wind dimension, R , is the scaling factor used to normalize the depth of the pit.

3. The user specifies the average height of emissions from the floor of the pit (H) and the pit volume (V). The effective pit depth (d_e) and the relative pit depth (D_r) are then calculated as follows:

$$d_e = V / (L \cdot W) \quad (1-72)$$

$$D_r = (d_e - H) / l \quad (1-73)$$

4. Based on observations and measurements in a wind tunnel study (Perry, et al., 1994), it is clear that the emissions within the pit are not uniformly released from the pit opening. Rather, the emissions show a tendency to be emitted primarily from an upwind sub-area of the pit opening. Therefore an effective area source (with A_e being the fractional size relative to the entire pit opening) is used to simulate the pit emissions. A_e represents a single area source whose dimensions and location depend on the effective depth of the pit and the wind direction. Based on wind tunnel results, if $D_r \geq 0.2$, then the effective area is about 8% of the total opening of the mine (i.e. $A_e = 0.08$). If $D_r < 0.2$, then the fractional area increases as follows:

$$A_e = (1.0 - 1.7 D_r^{1/3})^{1/2} \quad (1-74)$$

When $D_r = 0$, which means that the height of emissions above the floor equals the effective depth of the pit, the effective area is equal to the total area of the mine opening (i.e. $A_e = 1.0$).

Having determined the effective area from which the model will simulate the pit emissions, the specific dimensions of

this effective rectangular area are calculated as a function of θ such that (see Figure 1-10):

$$AW = A_e^{(1 - \cos^2 \theta)} \cdot W \quad (1-75)$$

and

$$AL = A_e^{(\cos^2 \theta)} \cdot L \quad (1-76)$$

Note that in equations 1-75 and 1-76, W is defined as the short dimension of the pit and L is the long dimension; AW is the dimension of the effective area aligned with the short side of the pit and AL is the dimension of the effective area aligned with the long side of the pit (see Figure 1-10). The dimensions AW and AL are used by the model to define the shape of the effective area for input to the area source algorithm described in Section 1.2.3.

The emission rate, Q_e , for the effective area is such that

$$Q_e = Q_a / A_e \quad (1-77)$$

where Q_a is the emission rate per unit area (from the pit after adjustment for escape fraction) if the emissions were uniformly released from the actual pit opening (with an area of $L \cdot W$). That is, if the effective area is one-third of the total area, then the emission rate (per unit area) used for the effective area is three times that from the full area.

Because of the high level of turbulence in the mine, the pollutant is initially mixed prior to exiting the pit. Therefore some initial vertical dispersion is included to represent this in the effective area source. Using the effective pit depth, d_e , as the representative dimension over which the pollutant is vertically mixed in the pit, the initial vertical dispersion value, σ_{z_0} , is equal to $d_e/4.3$. Note that $4.3\sigma_{z_0}$ represents about 90% of a Gaussian plume (in the vertical), so that the mixing in the pit is assumed to approximately equal the mixing in a plume.

Therefore, for the effective area source representing the pit emissions, the initial dispersion is included with ambient dispersion as:

$$\sigma_z = (\sigma_{z_0}^2 + \sigma_z^2(x))^{1/2} \quad (1-78)$$

For receptors close to the pit, the initial dispersion value can be particularly important.

Once the model has determined the characteristics of the effective area used to model pit emissions for a particular hour, the area source algorithm described in Section 1.2.3 is used to calculate the concentration or deposition flux values at the receptors being modeled.

1.3 THE ISC SHORT-TERM DRY DEPOSITION MODEL

1.3.1 General

This section describes the ISC Short Term dry deposition model, which is used to calculate the amount of material deposited (i.e., the deposition flux, F_d) at the surface from a particle plume through dry deposition processes.

The Short Term dry deposition model is based on a dry deposition algorithm developed by Venkatram (1998) as described in Section 1.1.6.3. This algorithm was selected after a review of several methods for treatment of dry deposition and settling of particulates.

The deposition flux, F_d , is calculated as the product of the concentration, P_d , and the sum of a deposition velocity, v_d , computed at a reference height z_d and the gravitational settling velocity, v_g :

$$F_d = P_d \cdot (v_d + v_g) \quad (1-79)$$

The concentration value, P_d , used in Equation (1-79) is calculated according to Equation (1-1) with deposition effects accounted for in the vertical term as described in Section 1.1.6.3. The calculation of the deposition and the gravitational settling velocities is described below.

1.3.2 Deposition and Gravitational Settling Velocities

A resistance method is used to calculate the deposition velocity, v_d . The general approach used in the resistance

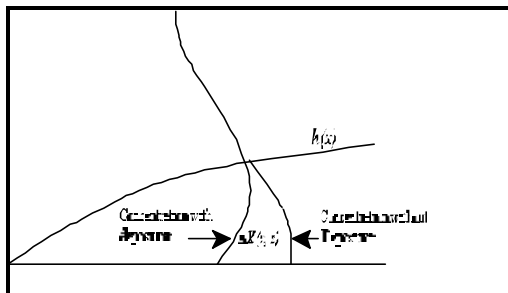
method is to include explicit parameterizations of the effects of Brownian motion and gravitational settling. The lowest few meters of the atmosphere can be divided into two layers: a fully turbulent region where vertical fluxes are nearly constant, and the thin quasi-laminar sublayer, i.e., the deposition layer. The resistance to transport through the turbulent, constant flux layer is the aerodynamic resistance (r_a), while the resistance to transport through the sublayer is the deposition layer resistance (r_d). In addition, the resistance to gravitational settling can be defined as the inverse of the gravitational settling velocity, i.e., ($1/v_g$). Note that r_a and r_d apply to the transport through the respective layers described above, while ($1/v_g$) applies to transport through all layers. This can be represented as follows:

(Note that r_a and r_d are in series, while ($1/v_g$) is a parallel resistance)

The total resistance, R, can be written as:

$$R = \frac{1}{r_a + r_d} + \frac{1}{v_g} \quad (1-80a)$$

From Section 1.1.6.3, dry deposition and



gravitational settling are treated as independent processes wherein the dry deposition is only dependent upon the resistances to transport through the various layers, and gravitational settling is only dependent upon v_g . Therefore, the deposition velocity (v_d) is defined as the inverse of the sum of resistances to pollutant transfer through various layers:

$$v_d = \frac{1}{r_a + r_d} \quad (1-80b)$$

where, v_d = the deposition velocity (cm/s),
 r_a = the aerodynamic resistance (s/cm), and,
 r_d = the deposition layer resistance (s/cm).

It is usually assumed that the eddy diffusivity for mass transfer within the turbulent, constant flux layer is similar to that for heat. The atmospheric resistance formulation is based on Byun and Dennis (1995):

stable ($L > 0$):

$$r_a = \frac{1}{k u_*} \left[\ln \left(\frac{z_d}{z_0} \right) + 4.7 \frac{z_d}{L} \right] \quad (1-81)$$

unstable ($L < 0$):

$$r_a = \frac{1}{k u_*} \left[\ln \frac{(\sqrt{1+16(z_d/|L|)} - 1)(\sqrt{1+16(z_0/|L|)} + 1)}{(\sqrt{1+16(z_d/|L|)} + 1)(\sqrt{1+16(z_0/|L|)} - 1)} \right] \quad (1-82)$$

where, u_* = the surface friction velocity (cm/s),
 k = the von Karman constant (0.4),
 z = the height above ground (m),
 L = the Monin-Obukhov length (m),
 z_d = deposition reference height (m), and
 z_o = the surface roughness length (m).

The coefficients used in the atmospheric resistance formulation are those suggested by Dyer (1974). A minimum value for L of 1.0m is used for rural locations. Recommended minimum values for urban areas are provided in the user's guides for the meteorological preprocessor programs PCRAMMET and MPRM.

The deposition layer resistance term is parameterized as per the approach used by Pleim et al. (1984) as follows:

$$r_d = \frac{1}{Sc^{-2/3} u_*} \quad (1-83)$$

where, Sc = the Schmidt number ($Sc = L/D_B$)
 (dimensionless),
 L = the viscosity of air ($\bullet 0.15 \text{ cm}^2/\text{s}$),
 D_B = the Brownian diffusivity (cm^2/s) of the
 pollutant in air,

The first term of Eqn. (1-83), involving the Schmidt number, parameterizes the effects of Brownian motion. The Brownian diffusivity of the pollutant (in cm²/s) is computed from the following relationship:

$$D_B = 8.09 \times 10^{-10} \left[\frac{T_a S_{CF}}{d_p} \right] \quad (1-84)$$

where, T_a = air temperature (°K),
 d_p = the particle diameter (:m),
 S_{CF} = the slip correction factor, which is computed as:

$$S_{CF} = 1. + \frac{2x_2 (a_1 + a_2 e^{- (a_3 d_p / x_2)})}{10^{-4} d_p} \quad (1-85)$$

and, x_2 , a_1 , a_2 , a_3 are constants with values of 6.5×10^{-6} , 1.257, 0.4, and 0.55×10^{-4} , respectively.

The gravitational settling velocity, v_g (cm/s), is calculated as:

$$v_g = \frac{(D - D_{AIR}) g d_p^2 c_2}{18\mu} S_{CF} \quad (1-86)$$

where, D = the particle density (g/cm³),
 D_{AIR} = the air density ($\bullet 1.2 \times 10^{-3}$ g/cm³),
 g = the acceleration due to gravity (981 cm/s²),

- : = the absolute viscosity of air ($\bullet 1.81 \times 10^{-4}$ g/cm/s), and
- c_2 = air units conversion constant (1×10^{-8} cm²/:m²).

The deposition algorithm also allows a small adjustment to the deposition rates to account for possible phoretic effects. Some examples of phoretic effects (Hicks, 1982) are:

THERMOPHORESIS: Particles close to a hot surface experience a force directed away from the surface because, on the average, the air molecules impacting on the side of the particle facing the surface are hotter and more energetic.

DIFFUSIOPHORESIS: Close to an evaporating surface, a particle is more likely to be impacted by water molecules on the side of the particle facing the surface. Since the water molecules have a lower molecular weight than the average air molecule, there is a net force toward the surface, which results in a small enhancement of the deposition velocity of the particle.

A second effect is that the impaction of new water vapor molecules at an evaporating surface displaces a certain volume of air. For example, 18 g of water vapor evaporating from 1 m² will displace 22.4 liters of air at standard temperature and pressure (STP) conditions (Hicks, 1982). This effect is called Stefan flow. The Stefan flow effect tends to reduce deposition fluxes from an evaporating surface. Conversely, deposition fluxes to a surface experiencing condensation will be enhanced.

ELECTROPHORESIS: Attractive electrical forces have the potential to assist the transport of small particles through the quasi-laminar deposition layer, and thus could increase the deposition velocity in situations with high local field strengths. However, Hicks (1982) suggests this effect is likely to be small in most natural circumstances.

Phoretic and Stefan flow effects are generally small. However, for particles in the range of 0.1 - 1.0 μm diameter, which have low deposition velocities, these effects may not always be negligible. Therefore, the ability to specify a phoretic term to the deposition velocity is added (i.e., $v_d^N = v_d + v_{d(\text{phor})}$, where v_d^N is the modified deposition velocity and $v_{d(\text{phor})}$ is the phoretic term).

Although the magnitude and sign of $v_{d(\text{phor})}$ will vary, a small, constant value of + 0.01 cm/s is used in the present implementation of the model to represent combined phoretic effects.

In addition to the mass mean diameters (microns), particle densities (gm/cm^3), and the mass fractions for each particle size category being modeled, the dry deposition model also requires surface roughness length (cm), friction velocity (m/s), and Monin-Obukhov length (m). The surface roughness length is specified by the user, and the meteorological preprocessor (PCRAMMET or MPRM) calculates the friction velocity and Monin-Obukhov length for input to the model.

1.3.3 Point and Volume Source Emissions

As stated in Equation (1-79), deposition is modeled as the product of the near-surface concentration (from Equation (1-1)) times the deposition velocity (from Equation (1-80b)). Therefore, the vertical term given in Equation (1-61) that is used to obtain the concentration at height z , subject to

particle settling and deposition, can be evaluated at ground level ($z=0$) for one particle size, and multiplied by a deposition velocity for that particle size to obtain a corresponding "vertical term" for deposition. Since more than one particle size category is typically used, the deposition for the n^{th} size category must also include the mass fraction for the category (N_n):

$$\begin{aligned}
 F_{dn} &= X_{dn} \cdot (v_{dn} + v_{gn}) \\
 &= \frac{Q_J K \phi_n (v_{dn} + v_{gn}) V_{dn}(x, z=0, h_{ed}) D}{2\pi \sigma_y \sigma_z u_s} \exp \left[-0.5 \left(\frac{y}{\sigma_y} \right)^2 \right]
 \end{aligned}
 \tag{1-87}$$

where K , V_d , and D were defined previously (Equations (1-1), (1-61), and (1-63)). The parameter Q_J is the total amount of material emitted during the time period J for which the deposition calculation is made. For example, Q_J is the total amount of material emitted during a 1-hour period if an hourly deposition is calculated. To simplify the user input, and to keep the maximum compatibility between input files for concentration and deposition runs, the model takes emission inputs in grams per second (g/s), and converts to grams per hour for deposition calculations. For time periods longer than an hour, the program sums the deposition calculated for each hour to obtain the total deposition flux for the period. In the case of a volume source, the user must specify the effective emission height h_e and the initial source dimensions F_{y_0} and F_{z_0} . It should be noted that for computational

purposes, the model calculates the quantity, $\sum_{n=1}^{NPD} \phi_n v_{dn} V_{dn}$, as the "vertical term."

1.3.4 Area and Open Pit Source Emissions

For area and open pit source emissions, Equation (1-65) is changed to the form:

$$\begin{aligned}
 F_{dn} &= \chi_{dn} \cdot (v_{dn} + v_{gn}) \\
 &= \frac{Q_{AJ} K \phi_n (v_{dn} + v_{gn})}{2 \pi U_s} \int_x \frac{V_{dn} D}{\sigma_y \sigma_z} \left(\int_y \exp \left[-0.5 \left(\frac{y}{\sigma_y} \right)^2 \right] \right) dy
 \end{aligned}
 \tag{1-88}$$

where K , V_a , D , and v_a are defined in Equations (1-1), (1-61), (1-63), and (1-80b). The parameter Q_{AJ} is the total mass per unit area emitted over the time period J for which deposition is calculated. The area source integral is estimated as described in Section 1.2.3.

1.4 THE ISC SHORT-TERM WET DEPOSITION MODEL

A scavenging ratio approach is used to model the deposition of gases and particles through wet removal. In this approach, the flux of material to the surface through wet deposition (F_w) is the product of a scavenging ratio times the concentration, integrated in the vertical:

$$F_w(x, y) = \int_0^{\infty} \Lambda \chi(x, y, z) dz
 \tag{1-89}$$

where the scavenging ratio (7) has units of s^{-1} . The concentration value is calculated using Equation (1-1). Since the precipitation is assumed to initiate above the plume height, a wet deposition flux is calculated even if the plume height exceeds the mixing height. Across the plume, the total flux to the surface must equal the mass lost from the plume so that

$$-\frac{d}{dx} Q(x) = \int_{-\infty}^{+\infty} F_v(x, y) dy = \Lambda Q(x) / u \quad (1-90)$$

Solving this equation for $Q(x)$, the source depletion relationship is obtained as follows:

$$Q(x) = Q_0 e^{-\Lambda x/u} = Q_0 e^{-\Lambda t} \quad (1-91)$$

where $t = x/u$ is the plume travel time in seconds. As with dry deposition (Section 1.3), the ratio $Q(x)/Q_0$ is computed as a wet depletion factor, which is applied to the flux term in Equation (1-89). The wet depletion calculation is also optional. Not considering the effects of wet depletion will result in conservative estimates of both concentration and deposition, since material deposited on the surface is not removed from the plume.

The scavenging ratio is computed from a scavenging coefficient and a precipitation rate (Scire et al., 1990):

$$\Lambda = \lambda \cdot R \quad (1-92)$$

where the coefficient **8** has units $(\text{s-mm/hr})^{-1}$, and the precipitation rate R has units (mm/hr) . The scavenging coefficient depends on the characteristics of the pollutant (e.g., solubility and reactivity for gases, size distribution for particles) as well as the nature of the precipitation (e.g., liquid or frozen). Jindal and Heinold (1991) have analyzed particle scavenging data reported by Radke et al. (1980), and found that the linear relationship of Equation (1-90) provides a better fit to the data than the non-linear assumption $7 = 8R^b$. Furthermore, they report best-fit values for **8** as a function of particle size. These values of the scavenging rate coefficient are displayed in Figure 1-11. Although the largest particle size included in the study is 10 μm , the authors suggest that **8** should reach a plateau beyond 10 μm , as shown in Figure 1-11. The scavenging rate coefficients for frozen precipitation are expected to be reduced to about 1/3 of the values in Figure 1-11 based on data for sulfate and nitrate (Scire et al., 1990). The scavenging rate coefficients are input to the model by the user.

The wet deposition algorithm requires precipitation type (liquid or solid) and precipitation rate, which is prepared for input to the model through the meteorological preprocessor programs (PCRAMMET or MPRM).

1.5 ISC COMPLEX TERRAIN SCREENING ALGORITHMS

The Short Term model uses a steady-state, sector-averaged Gaussian plume equation for applications in complex terrain (i.e., terrain above stack or release height). Terrain below release height is referred to as simple terrain; receptors located in simple terrain are modeled with the point source model described in Section 1.1. The sector average approach used in complex terrain implies that the lateral (crosswind) distribution of concentrations is uniform across a 22.5 degree sector. The complex terrain screening algorithms apply only to point source and volume source emissions; area source and open pit emission sources are excluded. The complex terrain point source model, which is based on the COMPLEX1 model, is described below. The description parallels the discussion for the simple terrain algorithm in Section 1.1, and includes the basic Gaussian sector-average equation, the plume rise formulas, and the formulas used for determining dispersion parameters.

1.5.1 The Gaussian Sector Average Equation

The Short Term complex terrain screening algorithm for stacks uses the steady-state, sector-averaged Gaussian plume equation for a continuous elevated source. As with the simple terrain algorithm described in Section 1.1, the origin of the source's coordinate system is placed at the ground surface at the base of the stack for each source and each hour. The x axis is positive in the downwind direction, the y axis is crosswind (normal) to the x axis and the z axis extends

vertically. The fixed receptor locations are converted to each source's coordinate system for each hourly concentration calculation. Since the concentrations are uniform across a 22.5 degree sector, the complex terrain algorithms use the radial distance between source and receptor instead of downwind distance. The calculation of the downwind, crosswind and radial distances is described in Section 1.5.2. The hourly concentrations calculated for each source at each receptor are summed to obtain the total concentration produced at each receptor by the combined source emissions.

For a Gaussian, sector-averaged plume, the hourly concentration at downwind distance x (meters) and crosswind distance y (meters) is given by:

$$X = \frac{Q K V D}{\sqrt{2\pi} R \Delta\theta' u_s \sigma_z} \cdot CORR \quad (1-93)$$

where:

- Q = pollutant emission rate (mass per unit time),
- K = units scaling coefficient (see Equation (1-1))
-) 2' = the sector width in radians (=0.3927)
- R = radial distance from the point source to the receptor = $[(x+x_y)^2 + y^2]^{1/2}$ (m)
- x = downwind distance from source center to receptor, measured along the plume axis (m)
- y = lateral distance from the plume axis to the receptor (m)

x_y = lateral virtual distance for volume sources (see Equation (1-35)), equals zero for point sources (m)

u_s = mean wind speed (m/sec) at stack height

F_z = standard deviation of the vertical concentration distribution (m)

V = the Vertical Term (see Section 1.1.6)

D = the Decay Term (see Section 1.1.7)

CORR = the attenuation correction factor for receptors above the plume centerline height (see Section 1.5.8)

Equation (1-93) includes a Vertical Term, a Decay Term, and a vertical dispersion term (F_z). The Vertical Term includes the effects of source elevation, receptor elevation, plume rise, limited vertical mixing, gravitational settling and dry deposition.

1.5.2 Downwind, Crosswind and Radial Distances

The calculation of downwind and crosswind distances is described in Section 1.1.2. Since the complex terrain algorithms in ISC are based on a sector average, the radial distance is used in calculating the plume rise (see Section 1.5.4) and dispersion parameters (see Section 1.5.5). The radial distance is calculated as $R = [x^2 + y^2]^{1/2}$, where x is the downwind distance and y is the crosswind distance described in Section 1.1.2.

1.5.3 Wind Speed Profile

See the discussion given in Section 1.1.3.

1.5.4 Plume Rise Formulas

The complex terrain algorithm in ISC uses the Briggs plume rise equations described in Section 1.1.4. For distances less than the distance to final rise, the complex terrain algorithm uses the distance-dependent plume height (based on the radial distance) as described in Section 1.1.4.10. Since the complex terrain algorithm does not incorporate the effects of building downwash, the Schulman-Scire plume rise described in Section 1.1.4.11 is not used for complex terrain modeling. The plume height is used in the calculation of the Vertical Term described in Section 1.5.6.

1.5.5 The Dispersion Parameters

The dispersion parameters used in the complex terrain algorithms of ISC are the same as the point source dispersion parameters for the simple terrain algorithms described in Section 1.1.5.1, except that the radial distance is used instead of the downwind distance. Since the lateral distribution of the plume in complex terrain is determined by the sector average approach, the complex terrain algorithm does not use the lateral dispersion parameter, F_y . The procedure to account for buoyancy-induced dispersion in the complex terrain algorithm only affects the vertical dispersion term (see Equation 1-48). Since the complex terrain algorithm does not incorporate the effects of building downwash, the enhanced dispersion parameters and virtual distances do not apply.

1.5.6 The Vertical Term

The Vertical Term used in the complex terrain algorithm in ISC is the same as described in Section 1.1.6 for the simple terrain algorithm, except that the plume height and dispersion parameter input to the vertical term are based on the radial distance, as described above, and that the adjustment of plume height for terrain above stack base is different, as described in Section 1.5.6.1.

1.5.6.1 The Vertical Term in Complex Terrain.

The ISC complex terrain algorithm makes the following assumption about plume behavior in complex terrain:

- The plume axis remains at the plume stabilization height above mean sea level as it passes over complex terrain for stable conditions (categories E and F), and uses a "half-height" correction factor for unstable and neutral conditions (categories A - D).
- The plume centerline height is never less than 10 m above the ground level in complex terrain.
- The mixing height is terrain following, i.e, the mixing height above ground at the receptor location is assumed to be the same as the height above ground at the source location.
- The wind speed is a function of height above the surface (see Equation (1-6)).

Thus, a modified plume stabilization height h_e' is substituted for the effective stack height h_e in the Vertical Term given by Equation (1-50). The effective plume stabilization height at the point x,y is given by:

$$h_e' = h_e - (1-F_T) H_t \quad (1-94)$$

where:

h_e = plume height at point x,y without terrain adjustment, as described in Section 1.5.4 (m)

$H_t = z_{(x,y)}^* - z_s$ = terrain height of the receptor location above the base of the stack (m)

$z_{(x,y)}^*$ = height above mean sea level of terrain at the receptor location (x,y) (m)

z_s = height above mean sea level of the base of the stack (m)

F_T = terrain adjustment factor, which is 0.5 for stability categories A - D and 0.0 for stability categories E and F.

The effect of the terrain adjustment factor is that the plume height relative to stack base is deflected upwards by an amount equal to half of the terrain height as it passes over complex terrain during unstable and neutral conditions. The plume height is not deflected by the terrain under stable conditions.

1.5.6.2 The Vertical Term for Particle Deposition

The Vertical Term for particle deposition used in the complex terrain algorithm in ISC is the same as described in Section 1.1.6 for the simple terrain algorithm, except that the plume height and dispersion parameter input to the vertical term are based on the radial distance, as described above, and that the adjustment of plume height for terrain above stack base is different, as described in Section 1.5.6.2.

1.5.7 The Decay Term

See the discussion given in Section 1.1.7.

1.5.8 The Plume Attenuation Correction Factor

Deflection of the plume by complex terrain features during stable conditions is simulated by applying an attenuation correction factor to the concentration with height in the sector of concern. This is represented by the variable CORR in Equation (1-93). The attenuation correction factor has a value of unity for receptors located at and below the elevation of the plume centerline in free air prior to encountering terrain effects, and decreases linearly with increasing height of the receptor above plume level to a value of zero for receptors located at least 400 m above the undisturbed plume centerline height. This relationship is shown in the following equation:

$$\begin{aligned}
 \text{CORR} &= 1.0 && \text{unstable/neutral} \\
 &= 1.0 && \Delta H_r \leq 0\text{m} \\
 &= 0.0 && \Delta H_r \geq 400\text{m} \\
 &= (400 - \Delta H_r) / 400 && \Delta H_r < 400\text{m}
 \end{aligned}
 \tag{1-95}$$

where:

CORR

= attenuation correction factor, which is between 0
and 1

)H_r

= height of receptor above undisturbed plume height, including height of receptor above local ground (i.e., flagpole height)

1.5.9 Wet Deposition in Complex Terrain

See the discussion given in Section 1.4.

1.6 ISC TREATMENT OF INTERMEDIATE TERRAIN

In the ISC Short Term model, intermediate terrain is defined as terrain that exceeds the height of the release, but is below the plume centerline height. The plume centerline height used to define whether a given receptor is on intermediate terrain is the distance-dependent plume height calculated for the complex terrain algorithm, before the terrain adjustment (Section 1.5.6.2) is applied.

If the plume height is equal to or exceeds the terrain height, then that receptor is defined as complex terrain for that hour and that source, and the concentration is based on the complex terrain screening algorithm only. If the terrain height is below the plume height but exceeds the physical release height, then that receptor is defined as intermediate terrain for that hour and source. For intermediate terrain receptors, concentrations from both the simple terrain algorithm and the complex terrain algorithm are obtained and the higher of the two concentrations is used for that hour and that source. If the terrain height is less than or equal to the physical release height, then that receptor is defined as simple terrain, and the concentration is based on the simple terrain algorithm only.

For deposition calculations, the intermediate terrain analysis is first applied to the concentrations at a given receptor, and the algorithm (simple or complex) that gives the highest concentration at that receptor is used to calculate the deposition value.

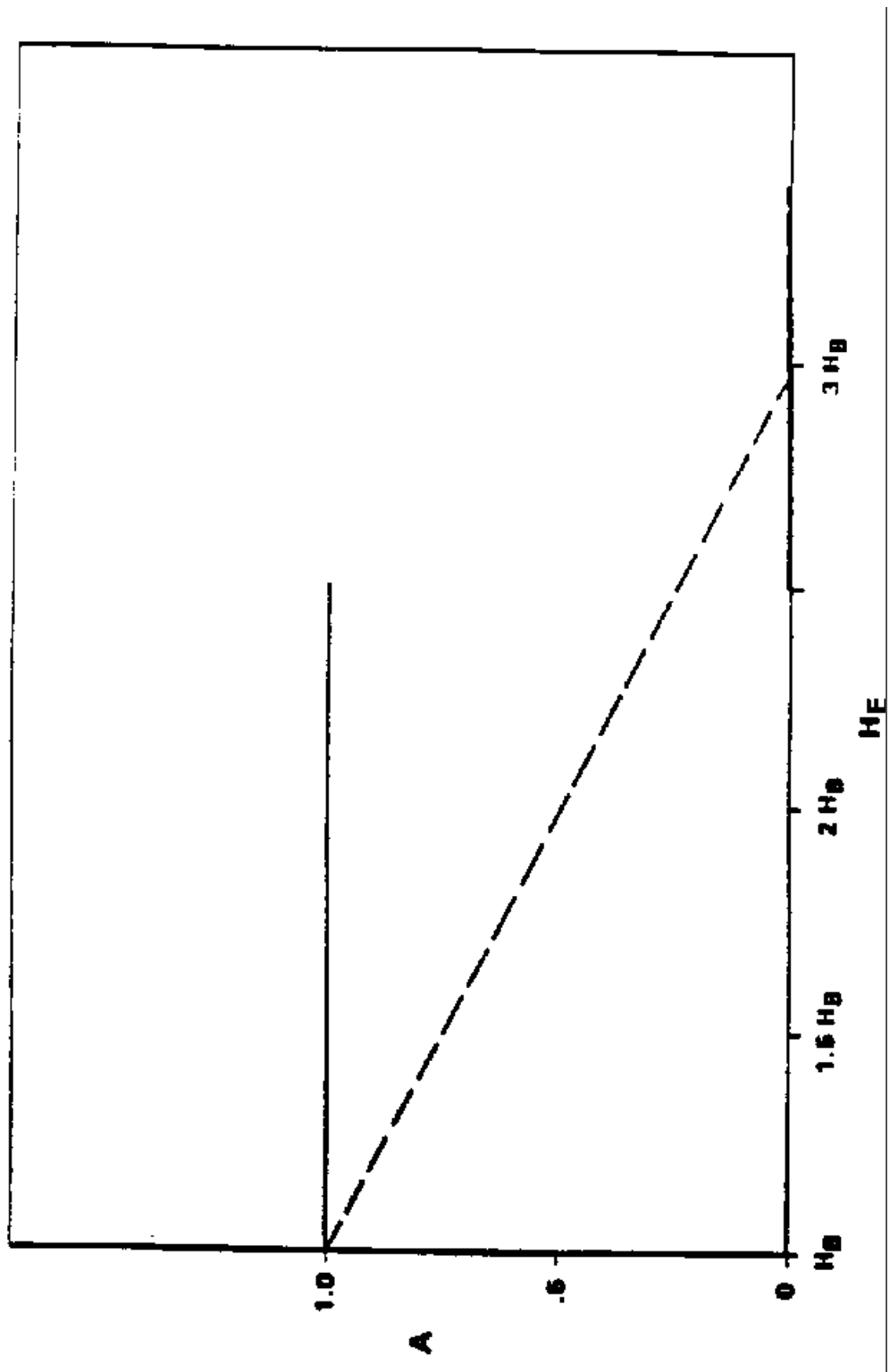
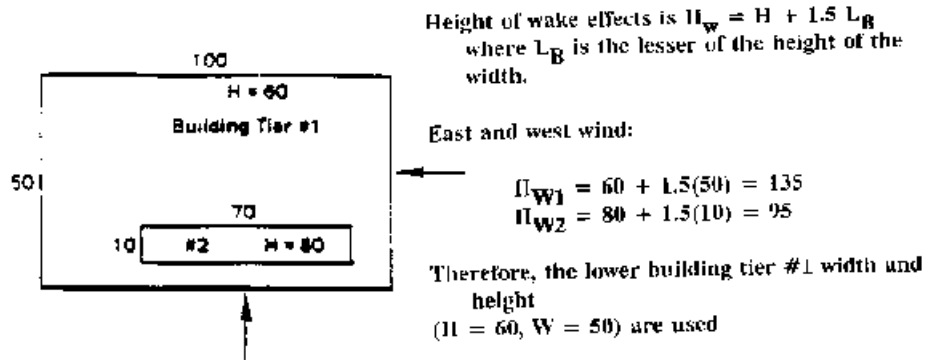


FIGURE 1-1. LINEAR DECAY FACTOR, A AS A FUNCTION OF EFFECTIVE STACK HEIGHT, H_e . A SQUAT BUILDING IS ASSUMED FOR SIMPLICITY.



Height of wake effects is $H_w = H + 1.5 L_B$ where L_B is the lesser of the height of the width.

East and west wind:

$$H_{w1} = 60 + 1.5(50) = 135$$

$$H_{w2} = 80 + 1.5(10) = 95$$

Therefore, the lower building tier #1 width and height ($H = 60, W = 50$) are used

North and South wind:

$$H_{w1} = 60 + 1.5(60) = 150$$

$$H_{w2} = 80 + 1.5(70) = 185$$

Therefore, the upper building tier #2 width and height ($H = 80, W = 70$) are used

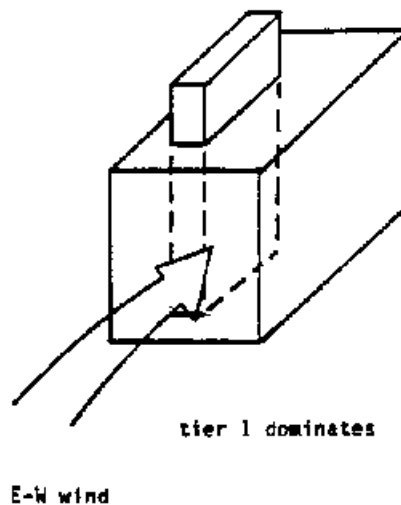
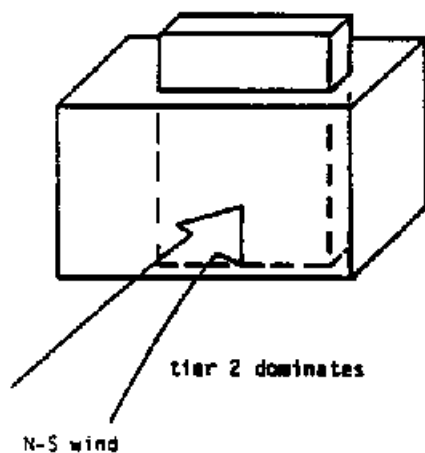


FIGURE 1-2. ILLUSTRATION OF TWO TIERED BUILDING WITH DIFFERENT TIERS DOMINATING DIFFERENT WIND DIRECTIONS

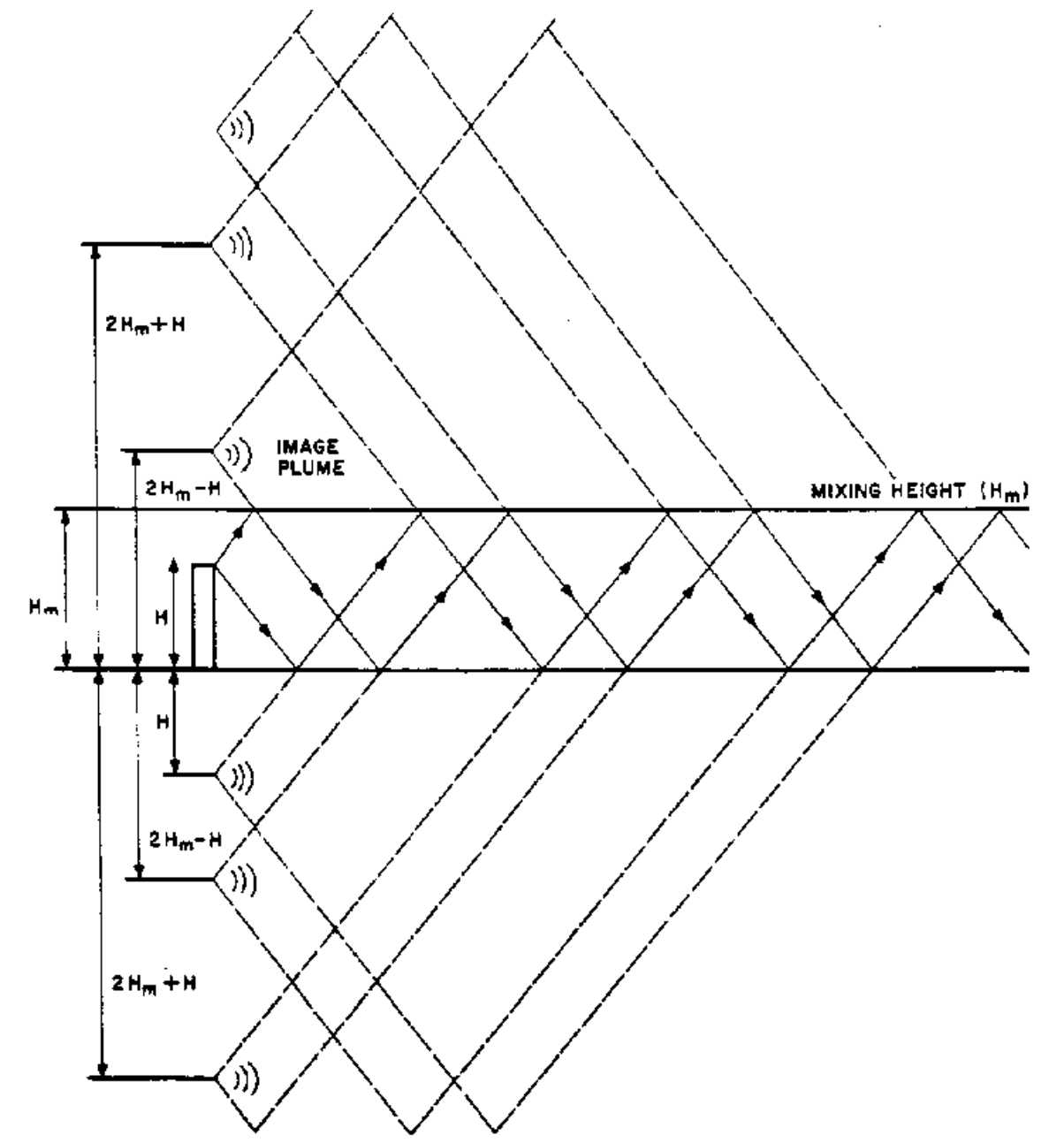


FIGURE 1-3. THE METHOD OF MULTIPLE PLUME IMAGES USED TO SIMULATE PLUME REFLECTION IN THE ISC2 MODEL

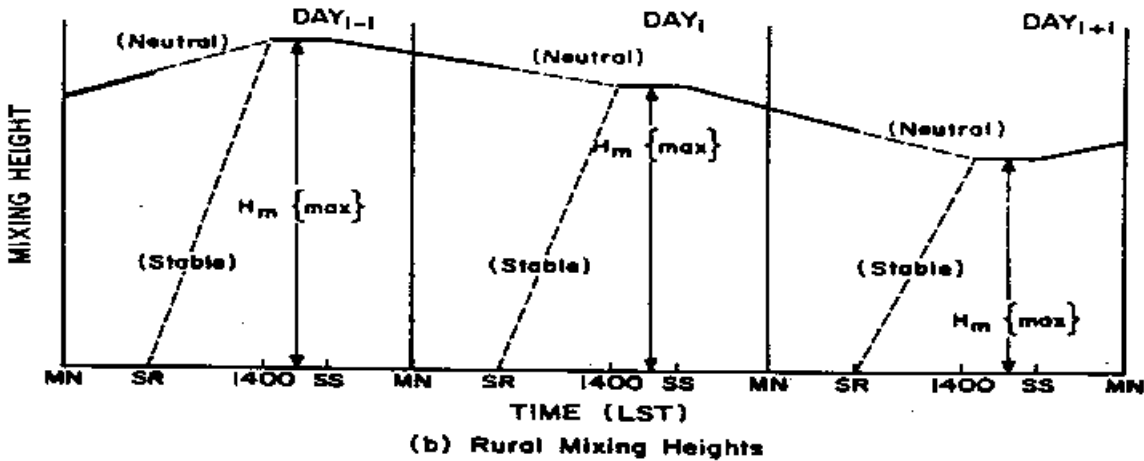
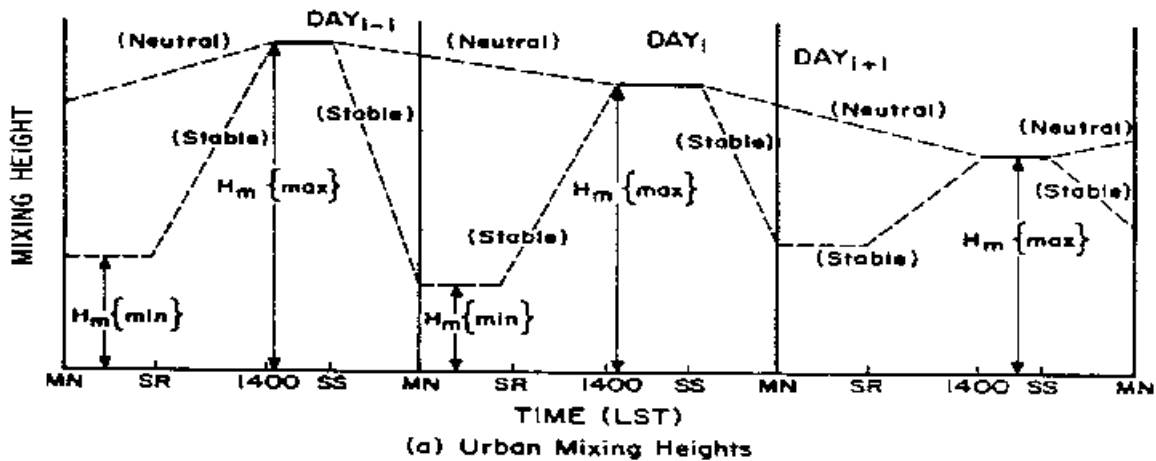


FIGURE 1-4. SCHEMATIC ILLUSTRATION OF (a) URBAN AND (b) RURAL MIXING HEIGHT INTERPOLATION PROCEDURES

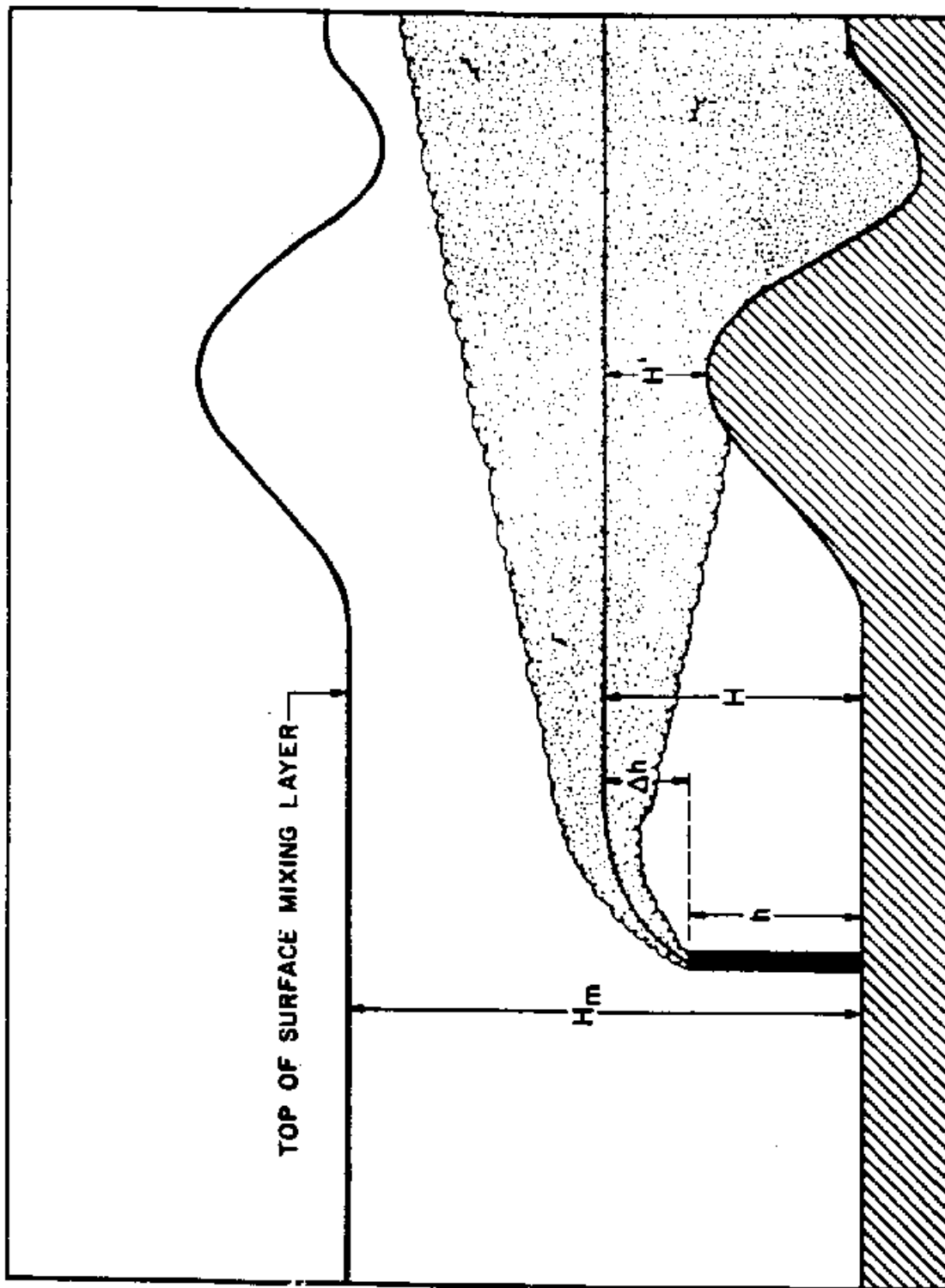


FIGURE 1-5. ILLUSTRATION OF PLUME BEHAVIOR IN ELEVATED TERRAIN ASSUMED BY THE ISC2 MODEL

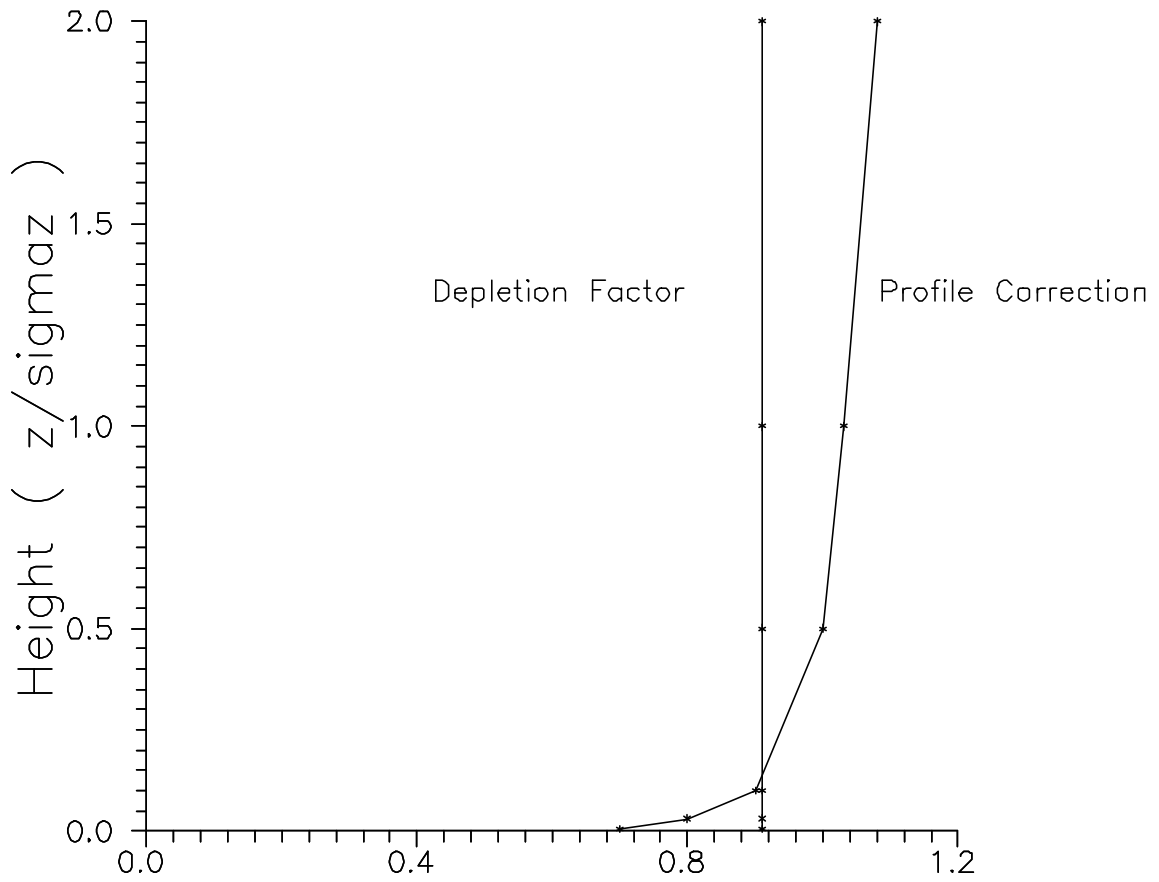


FIGURE 1-6. ILLUSTRATION OF THE DEPLETION FACTOR F_0 AND THE CORRESPONDING CORRECTION FACTOR $P(x, z)$.

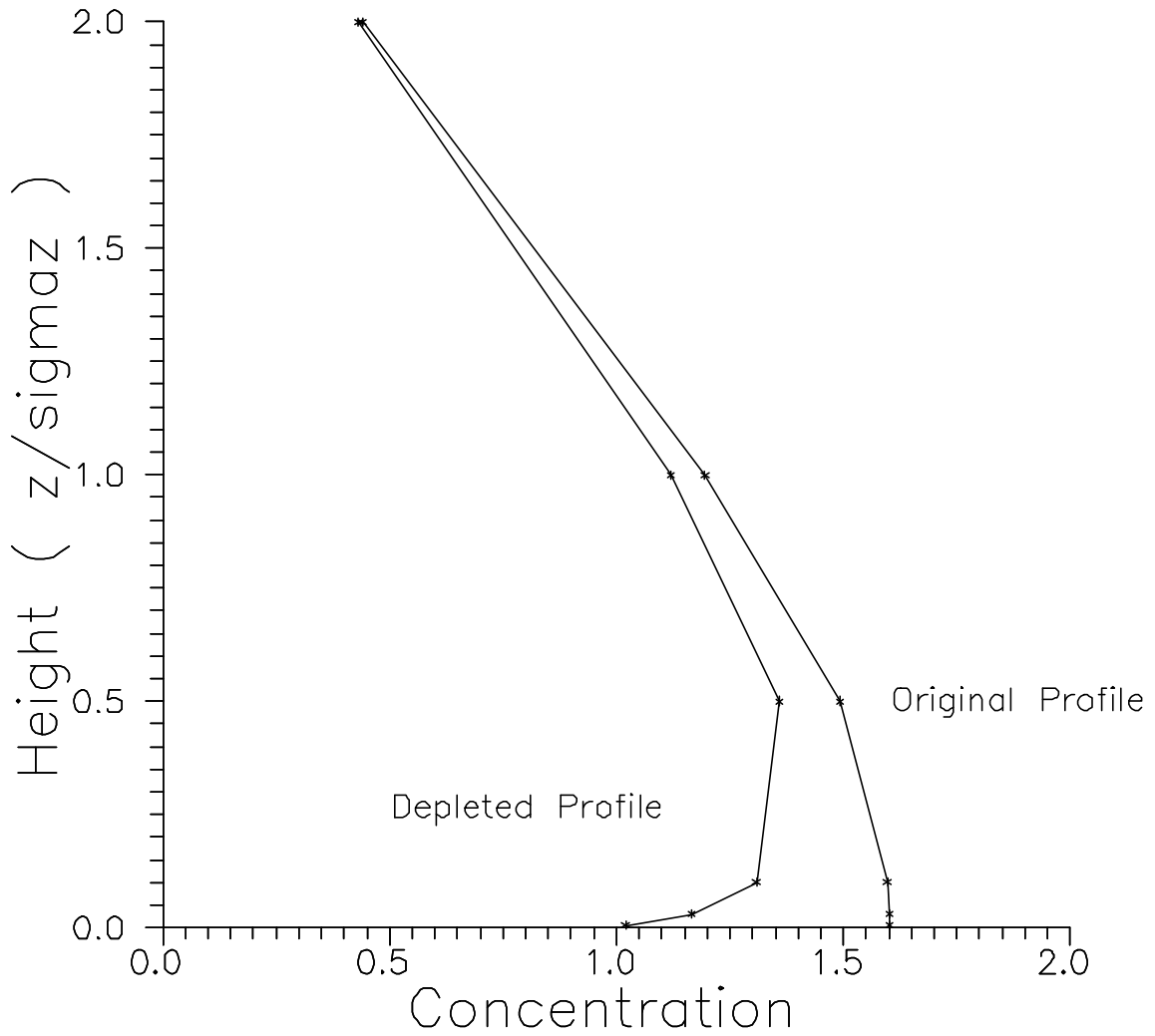
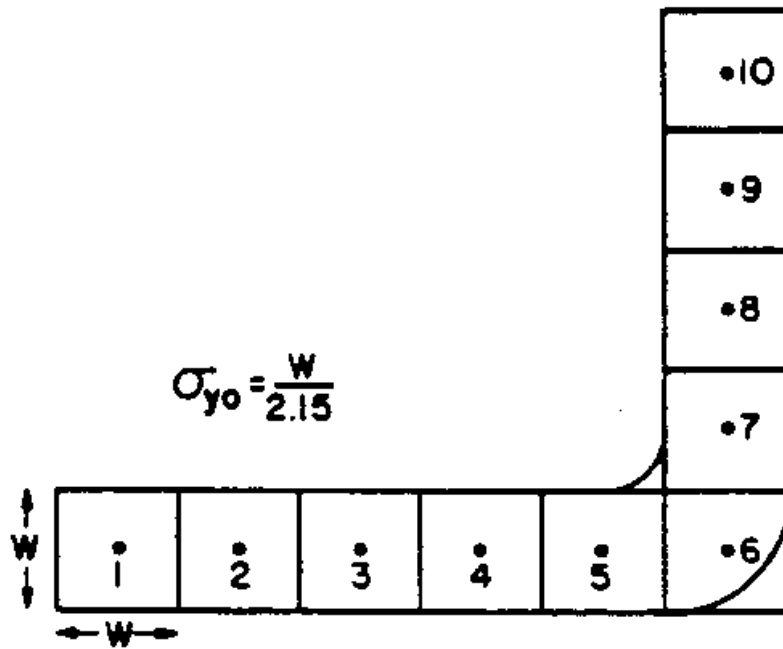
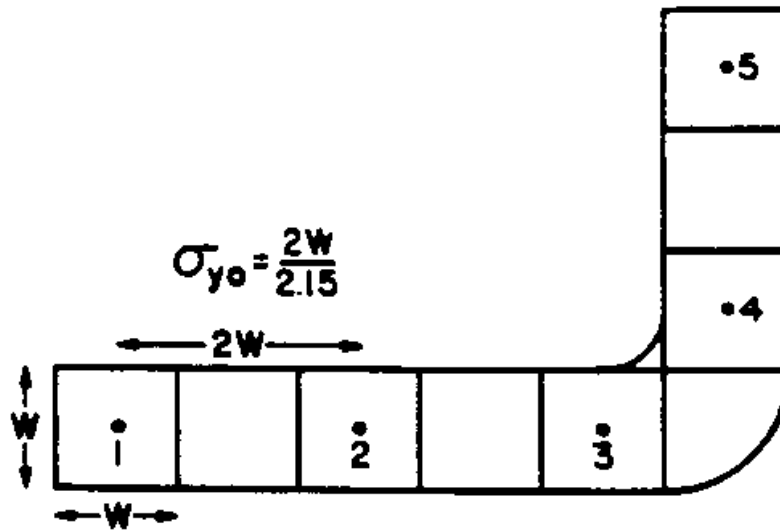


FIGURE 1-7. VERTICAL PROFILE OF CONCENTRATION BEFORE AND AFTER APPLYING $P(x, z)$ SHOWN IN

FIGURE 1-6.



(a) EXACT REPRESENTATION



(b) APPROXIMATE REPRESENTATION

FIGURE 1-8. EXACT AND APPROXIMATE REPRESENTATIONS OF A LINE SOURCE BY MULTIPLE VOLUME SOURCES

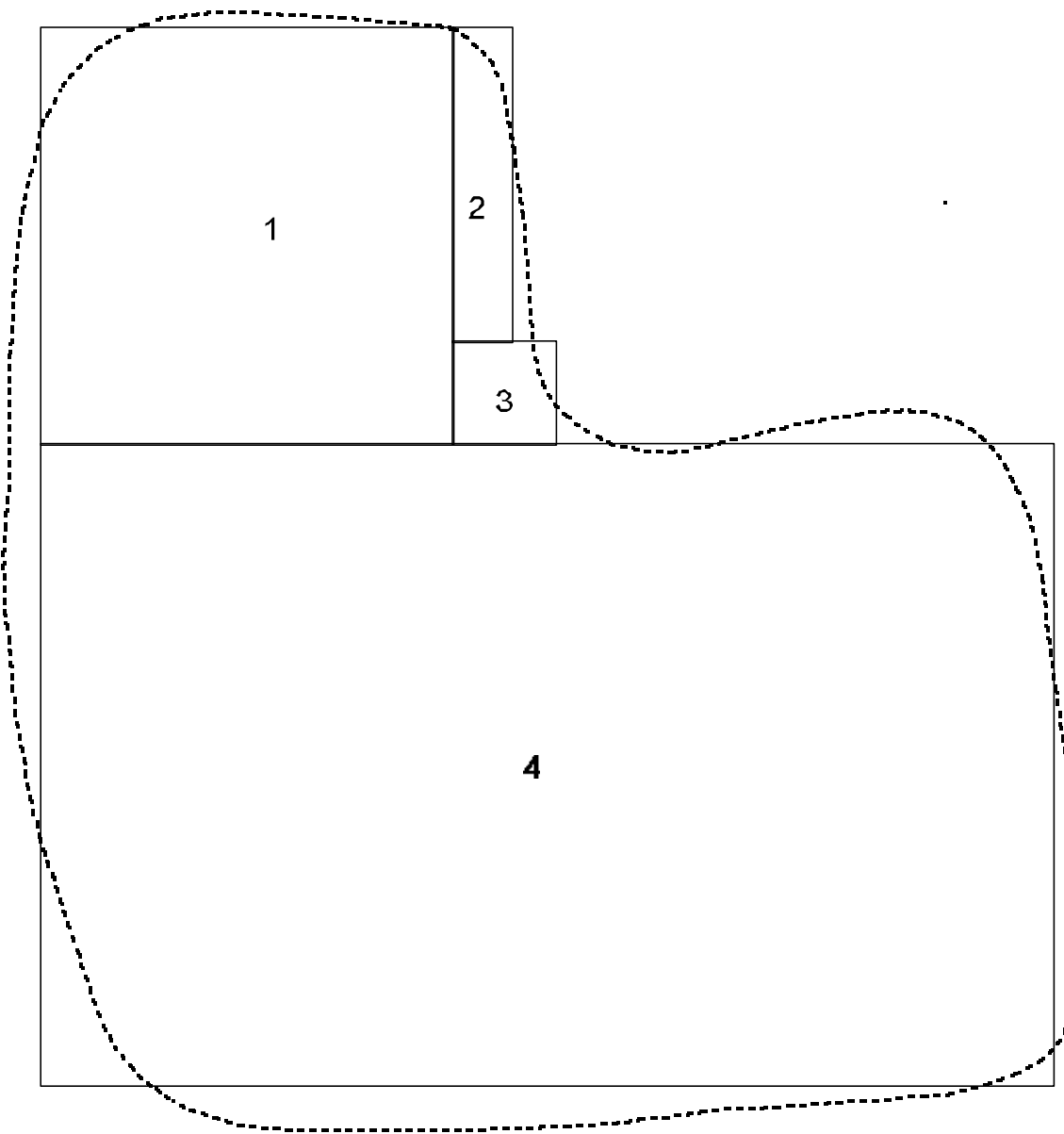


FIGURE 1-9. REPRESENTATION OF AN IRREGULARLY SHAPED AREA SOURCE BY 4 RECTANGULAR AREA SOURCES

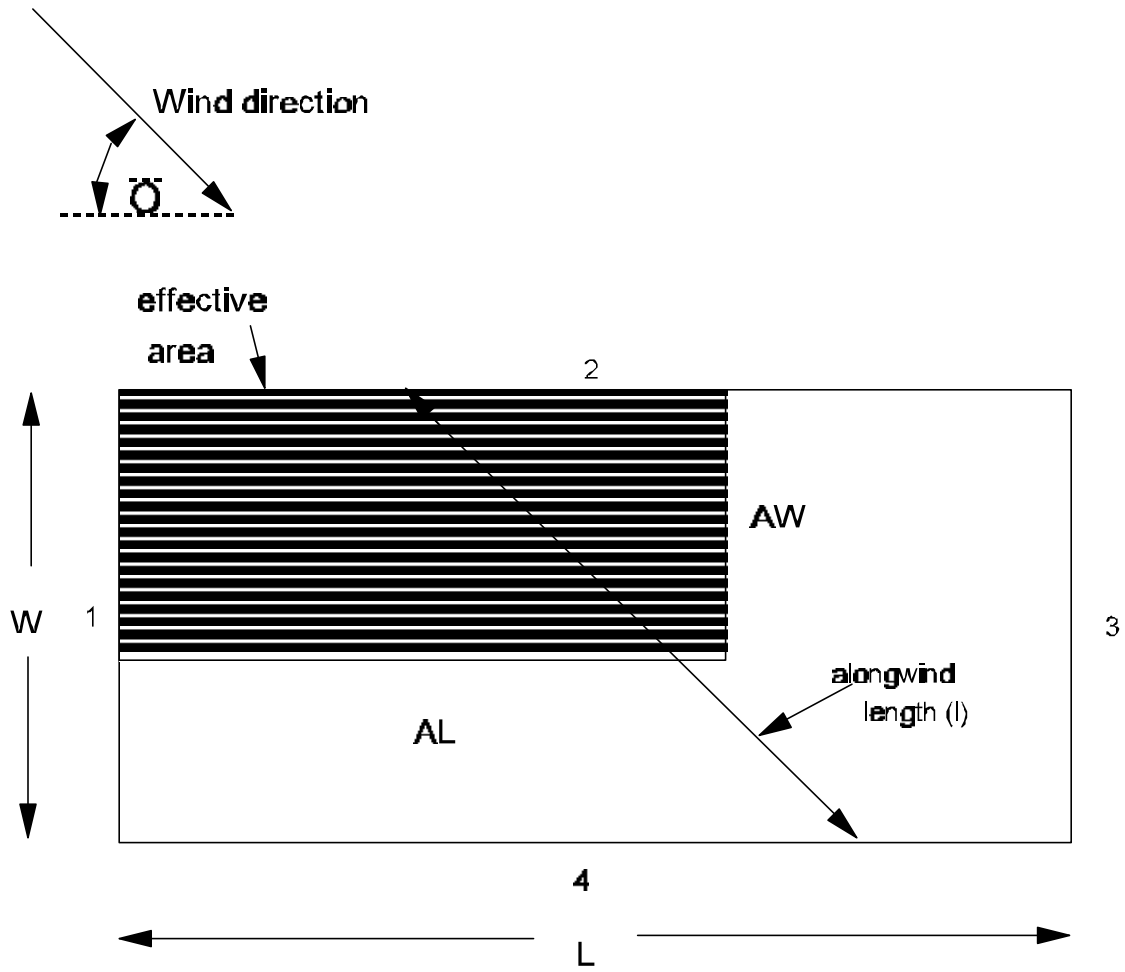


FIGURE 1-10. EFFECTIVE AREA AND ALONGWIND WIDTH FOR AN OPEN PIT SOURCE

Wet Scavenging Rate Coefficient (10^{-4}s^{-1})/mm-h⁻¹

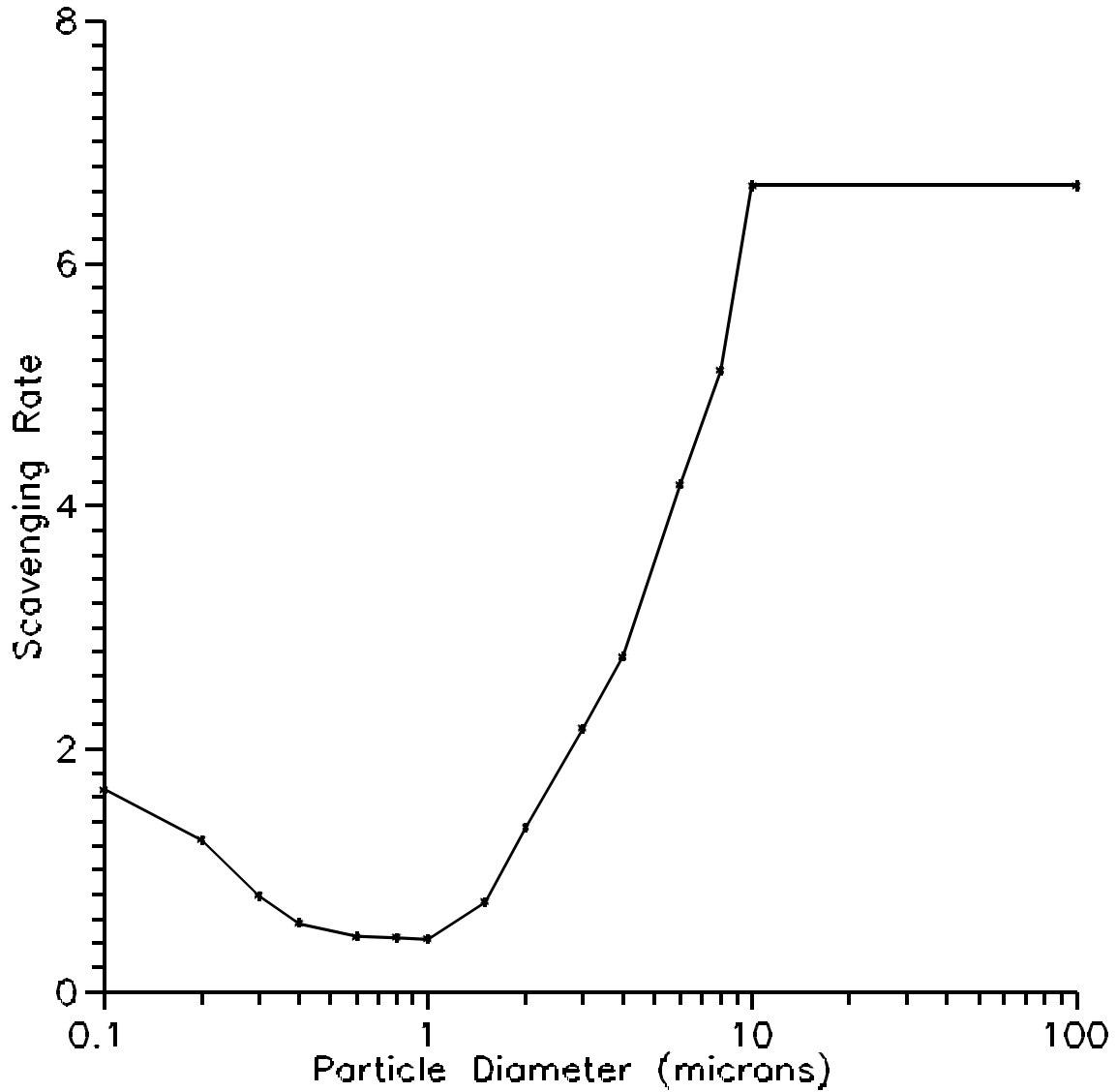


FIGURE 1-11. WET SCAVENGING RATE COEFFICIENT AS A FUNCTION OF PARTICLE SIZE (JINDAL & HEINOLD, 1991)

2.0 THE ISC LONG-TERM DISPERSION MODEL EQUATIONS

This section describes the ISC Long-Term model equations. Where the technical information is the same, this section refers to the ISC Short-Term model description in Section 1 for details. The long-term model provides options for modeling the same types of sources as provided by the short-term model. The information provided below follows the same order as used for the short-term model equations.

The ISC long-term model uses input meteorological data that have been summarized into joint frequencies of occurrence for particular wind speed classes, wind direction sectors, and stability categories. These summaries, called STAR summaries for STability ARray, may include frequency distributions over a monthly, seasonal or annual basis. The long term model has the option of calculating concentration or dry deposition values for each separate STAR summary input and/or for the combined period covered by all available STAR summaries. Since the wind direction input is the frequency of occurrence over a sector, with no information on the distribution of winds within the sector, the ISC long-term model uses a Gaussian sector-average plume equation as the basis for modeling pollutant emissions on a long-term basis.

2.1 POINT SOURCE EMISSIONS

2.1.1 The Gaussian Sector Average Equation

The ISC long-term model makes the same basic assumption as the short-term model. In the long-term model, the area surrounding a continuous source of pollutants is divided into sectors of equal angular width corresponding to the sectors of the seasonal and annual frequency distributions of wind direction, wind speed, and stability. Seasonal or annual emissions from the source are partitioned among the sectors according to the frequencies of wind blowing toward the sectors. The concentration fields calculated for each source are translated to a common coordinate system (either polar or Cartesian as specified by the user) and summed to obtain the total due to all sources.

For a single stack, the mean seasonal concentration is given by:

$$X_1 = \frac{K}{\sqrt{2\pi} R \Delta \theta'} \sum_{i,j,k} \frac{Q f S V D}{u_s \sigma_z} \quad (2-1)$$

where:

K = units scaling coefficient (see Equation (1-1))

Q = pollutant emission rate (mass per unit time), for the i^{th} wind-speed category, the k^{th} stability category and the l^{th} season

f = frequency of occurrence of the i^{th} wind-speed category, the j^{th} wind-direction category and the k^{th} stability category for the l^{th} season

- θ = the sector width in radians
- R = radial distance from lateral virtual point source (for building downwash) to the receptor = $[(x+x_y)^2 + y^2]^{1/2}$ (m)
- x = downwind distance from source center to receptor, measured along the plume axis (m)
- y = lateral distance from the plume axis to the receptor (m)
- x_y = lateral virtual distance (see Equation (1-35)), equals zero for point sources without building downwash, and for downwash sources that do not experience lateral dispersion enhancement (m)
- S = a smoothing function similar to that of the AQDM (see Section 2.1.8)
- u_s = mean wind speed (m/sec) at stack height for the i^{th} wind-speed category and k^{th} stability category
- F_z = standard deviation of the vertical concentration distribution (m) for the k^{th} stability category
- V = the Vertical Term for the i^{th} wind-speed category, k^{th} stability category and l^{th} season
- D = the Decay Term for the i^{th} wind speed category and k^{th} stability category

The mean annual concentration at the point (r, θ) is calculated from the seasonal concentrations using the expression:

$$\chi_a = 0.25 \sum_{i=1}^4 \chi_i \quad (2-2)$$

The terms in Equation (2-1) correspond to the terms discussed in Section 1.1 for the short-term model except that the parameters are defined for discrete categories of wind-speed, wind-direction, stability and season. The various terms are briefly discussed in the following subsections. In addition to point source emissions, the ISC long-term concentration model considers emissions from volume and area sources. These model options are discussed in Section 2.2. The optional algorithms for calculating dry deposition are discussed in Section 2.3.

2.1.2 Downwind and Crosswind Distances

See the discussion given in Section 1.1.2.

2.1.3 Wind Speed Profile

See the discussion given in Section 1.1.3.

2.1.4 Plume Rise Formulas

See the discussion given in Section 1.1.4.

2.1.5 The Dispersion Parameters

2.1.5.1 Point Source Dispersion Parameters.

See Section 1.1.5.1 for a discussion of the procedures use to calculate the standard deviation of the vertical concentration distribution F_z for point sources (sources

without initial dimensions). Since the long term model assumes a uniform lateral distribution across the sector width, the model does not use the standard deviation of the lateral dispersion, F_y (except for use with the Schulman-Scire plume rise formulas described in Section 1.1.4.11).

2.1.5.2 Lateral and Vertical Virtual Distances.

See Section 1.1.5.2 for a discussion of the procedures used to calculate vertical virtual distances. The lateral virtual distance is given by:

$$x_y = r_o \cot\left(\frac{\Delta\theta'}{2}\right) \quad (2-3)$$

where r_o is the effective source radius in meters. For volume sources (see Section 2.2.2), the program sets r_o equal to $2.15F_{y0}$, where F_{y0} is the initial lateral dimension. For area sources (see Section 2.2.3), the program sets r_o equal to $x_o/\sqrt{\pi}$ where x_o is the length of the side of the area source. For plumes affected by building wakes (see Section 1.1.5.2), the program sets r_o equal to $2.15 F_y'$ where F_y' is given for squat buildings by Equation (1-41), (1-42), or (1-43) for downwind distances between 3 and 10 building heights and for tall buildings by Equation (1-44) for downwind distances between 3 and 10 building widths. At downwind distances greater than 10 building heights for Equation (1-41), (1-42), or (1-43), F_y' is held constant at the value of F_y' calculated at a downwind distance of 10 building heights. Similarly, at downwind distances greater than 10 building widths for

Equation (1-44), F_y' is held constant at the value of F_y' calculated at a downwind distance of 10 building widths.

2.1.5.3 Procedures Used to Account for the Effects of Building Wakes on Effluent Dispersion.

With the exception of the equations used to calculate the lateral virtual distance, the procedures used to account for the effects of building wake effects on effluent dispersion are the same as those outlined in Section 1.1.5.3 for the short-term model. The calculation of lateral virtual distances by the long-term model is discussed in Section 2.1.5.2 above.

2.1.5.4 Procedures Used to Account for Buoyancy-Induced Dispersion.

See the discussion given in Section 1.1.5.4.

2.1.6 The Vertical Term

2.1.6.1 The Vertical Term for Gases and Small Particulates.

Except for the use of seasons and discrete categories of wind-speed and stability, the Vertical Term for gases and small particulates corresponds to the short term version discussed in Section 1.1.6. The user may assign a separate mixing height z_i to each combination of wind-speed and stability category for each season.

As with the Short-Term model, the Vertical Term is changed to the form:

$$V = \frac{\sqrt{2\pi}\sigma_z}{z_i} \quad (2-4)$$

at downwind distances where the F_z/z_i ratio is greater than or equal to 1.6. Additionally, the ground-level concentration is set equal to zero if the effective stack height h_e exceeds the mixing height z_i . As explained in Section 1.1.6.1, the ISC model currently assumes unlimited mixing for the E and F stability categories.

2.1.6.2 The Vertical Term in Elevated Terrain.

See the discussion given in Section 1.1.6.2.

2.1.6.3 The Vertical Term for Large Particulates.

Section 1.1.6.3 discusses the differences in the dispersion of large particulates and the dispersion of gases and small particulates and provides the guidance on the use of this option. The Vertical Term for large particulates is given by Equation (1-53).

2.1.7 The Decay Term

See the discussion given in Section 1.1.7.

2.1.8 The Smoothing Function

As shown by Equation (2-1), the rectangular concentration distribution within a given angular sector is modified by the function $S\{\theta\}$ which smooths discontinuities in the concentration at the boundaries of adjacent sectors. The centerline concentration in each sector is unaffected by contribution from adjacent sectors. At points off the sector centerline, the concentration is a weighted function of the concentration at the centerline and the concentration at the centerline of the nearest adjoining sector. The smoothing function is given by:

$$S = \frac{(\Delta\theta' - |\theta_j' - \theta'|)}{\Delta\theta'} \quad \text{for } |\theta_j' - \theta'| \leq \Delta\theta' \tag{2-5}$$

or

$$= 0 \quad \text{for } |\theta_j' - \theta'| > \Delta\theta'$$

where:

θ_j' = the angle measured in radians from north to the centerline of the j^{th} wind-direction sector

θ' = the angle measured in radians from north to the receptor point (R, θ) where R, defined above for equation 2-1, is measured from the lateral virtual source.

2.2 NON-POINT SOURCE EMISSIONS

2.2.1 General

As explained in Section 1.2.1, the ISC volume, area and open pit sources are used to simulate the effects of emissions from a wide variety of industrial sources. Section 1.2.2 provides a description of the volume source model, Section 1.2.3 provides a description of the area source model, and Section 1.2.4 provides a description of the open pit model. The following subsections give the volume, area and open pit source equations used by the long-term model.

2.2.2 The Long-Term Volume Source Model

The ISC Long Term Model uses a virtual point source algorithm to model the effects of volume sources. Therefore, Equation (2-1) is also used to calculate seasonal average ground-level concentrations for volume source emissions. The user must assign initial lateral (F_{y_0}) and vertical (F_{z_0}) dimensions and the effective emission height h_e . A discussion of the application of the volume source model is given in Section 1.2.2.

2.2.3 The Long-Term Area Source Model

The ISC Long Term Area Source Model is based on the numerical integration algorithm for modeling area sources used by the ISC Short Term model, which is described in detail in Section 1.2.3. For each combination of wind speed class, stability category and wind direction sector in the STAR meteorological frequency summary, the ISC Long Term model calculates a sector average concentration by integrating the results from the ISC Short Term area source algorithm across the sector. A trapezoidal integration is used, as follows:

$$\bar{X}_i = \frac{\int f(\theta) X(\theta) d\theta}{S} = \frac{1}{N} \left[\sum_{j=1}^{N-1} f_{ij} X(\theta_{ij}) + \frac{(f_{i1} X(\theta_{i1}) + f_{iN} X(\theta_{iN}))}{2} \right] + e(\theta) \quad (2-6a)$$

$$e(\theta) = \frac{\overline{X_{NEW}} - \overline{X_{OLD}}}{\overline{X_{mid}}} ; \quad \overline{X_{mid}} = \frac{\overline{X_{NEW}} + \overline{X_{OLD}}}{2} \quad (2-6b)$$

where:

- P_i = the sector average concentration value for the i^{th} sector
- S = the sector width
- f_{ij} = the frequency of occurrence for the j^{th} wind direction in the i^{th} sector

- ϵ = the error term - a criterion of $\epsilon < 2$ percent is used to check for convergence of the sector average calculation
- $P(\theta_{ij})$ = the concentration value, based on the numerical integration algorithm using Equation (1-58) for the j^{th} wind direction in the i^{th} sector
- θ_{ij} = the j^{th} wind direction in the i^{th} sector, $j = 1$ and N correspond to the two boundaries of the sector.

The application of Equation (2-6a) to calculate the sector average concentration from area sources is an iterative process. Calculations using the ISC Short Term algorithm (Equation (1-58)) are initially made for three wind directions, corresponding to the two boundaries of the sector and the centerline direction. The algorithm then calculates the concentration for wind directions midway between the three directions, for a total of five directions, and calculates the error term. If the error is less than 2 percent, then the concentration based on five directions is used to represent the sector average, otherwise, additional wind directions are selected midway between each of the five directions and the process continued. This process continues until the convergence criteria, described below, are satisfied.

In order to avoid abrupt changes in the concentrations at the sector boundaries with the numerical integration algorithm, a linear interpolation is used to determine the frequency of occurrence of each wind direction used for the individual simulations within a sector, based on the frequencies of occurrence in the adjacent sectors. This "smoothing" of the frequency distribution has a similar

effect as the smoothing function used for the ISC Long Term point source algorithm, described in Section 2.1.8. The frequency of occurrence of the j^{th} wind direction between sectors i and $i+1$ can be calculated as:

$$f_{ij} = F_i + (\theta_{i+1} - \theta_{ij}) \frac{(F_{i+1} - F_i)}{(\theta_{i+1} - \theta_i)} \quad (2-6c)$$

where:

- F_i = the frequency of occurrence for the i^{th} sector
- F_{i+1} = the frequency of occurrence for the $i+1^{\text{th}}$ sector
- θ_i = the central wind direction for the i^{th} sector
- θ_{i+1} = the central wind direction for the $i+1^{\text{th}}$ sector
- θ_{ij} = the specific wind direction between θ_i and θ_{i+1}
- f_{ij} = the interpolated (smoothed) frequency of occurrence for the specific wind direction θ_{ij}

The ISCLT model uses a set of three criteria to determine whether the process of calculating the sector average concentration has "converged." The calculation process will be considered to have converged, and the most recent estimate of the trapezoidal integral used, if any of the following conditions is true:

- 1) if the number of "halving intervals" (N) in the trapezoidal approximation of the sector average has reached 10, where the number of individual elements in the approximation is given by $1 + 2^{N-1} = 513$ for N of 10;

- 2) if the estimate of the sector average has converged to within a tolerance of 0.02 (i.e., 2 percent), for two successive iterations, and at least 2 halving intervals have been completed (a minimum of 5 wind direction simulations); or
- 3) if the estimate of the sector average concentration is less than $1.0E-10$, and at least 2 halving intervals have been completed.

The first condition essentially puts a time limit on the integration process, the second condition checks for the accuracy of the estimate of the sector average, and the third condition places a lower threshold limit that avoids convergence problems associated with very small concentrations where truncation error may be significant.

2.2.4 The Long-Term Open Pit Source Model

The ISC Long Term Open Pit Source Model is based on the use of the long term area source model described in Section 2.2.3. The escape fractions and adjusted mass distribution for particle emissions from an open pit, and the determination of the size, shape and location of the effective area source used to model open pit emissions are described in Section 1.2.4. For the Long Term model, a sector average value for open pit sources is calculated by determining an effective area for a range of wind directions within the sector and increasing the number of wind directions used until the result converges, as described in Section 2.2.3 for the Long Term area source model. The contribution from each effective area used within a sector is calculated using the Short Term area source model described in Section 1.2.3.

2.3 THE ISC LONG-TERM DRY DEPOSITION MODEL

2.3.1 General

The concepts upon which the ISC long-term dry deposition model are based are discussed in Sections 1.1.6.3 and 1.3.

2.3.2 Point and Volume Source Emissions

The seasonal deposition at the point located at a particular distance (r) and direction (θ) with respect to the base of a stack or the center of a volume source for particulates in the n^{th} particle size category is given by:

$$F_{d\ 1,n} = \frac{K \phi_n}{\sqrt{2\pi R^2 \Delta\theta'}} \sum_{i,j,k} \frac{Q_i f S V_{dn} D}{\sigma_z} \quad (2-7)$$

where the vertical term for deposition, V_{dn} , was defined in Section 1.3.2. K and D are described in Equations (1-1) and (1-63), respectively. Q_j is the product of the total time during the l^{th} season, of the seasonal emission rate Q for the i^{th} wind-speed category, k^{th} stability category. For example, if the emission rate is in grams per second and there are 92 days in the summer season (June, July, and August), $Q_{j,1-3}$ is given by $7.95 \times 10^6 Q_{1-3}$. It should be noted that the user need not vary the emission rate by season or by wind speed and stability. If an annual average emission rate is assumed, Q_j is equal to $3.15 \times 10^7 Q$ for a 365-day year. For a plume comprised of N particle size categories, the total seasonal deposition is obtained by summing Equation (2-7) over the N particle size categories. The program also sums the seasonal deposition values to obtain the annual deposition.

2.3.3 Area and Open Pit Source Emissions

The area and open pit source dry deposition calculations for the ISCLT model are based on the numerical integration algorithm for modeling area sources used by the ISCST model. Section 1.3.4, Equation (1-88), describes the numerical integration for the Short Term model that is applied to specific wind directions by the Long Term model in a trapezoidal integration to calculate the sector average. The process of calculating sector averages for area sources in the Long Term model is described by Equation (2-6) in Section 2.2.3.

3.0 REFERENCES

- Bowers, J.F., J.R. Bjorklund and C.S. Cheney, 1979:
Industrial Source Complex (ISC) Dispersion Model
User's Guide. Volume I, EPA-450/4-79-030, U.S.
Environmental Protection Agency, Research Triangle
Park, North Carolina 27711.
- Bowers, J.R., J.R. Bjorklund and C.S. Cheney, 1979:
Industrial Source Complex (ISC) Dispersion Model
User's Guide. Volume II, EPA-450/4-79-031, U.S.
Environmental Protection Agency, Research Triangle
Park, North Carolina 27711.
- Briggs, G.A., 1969, Plume Rise, USAEC Critical Review
Series, TID-25075, National Technical Information
Service, Springfield, Virginia 22161.
- Briggs, G.A., 1979: Some Recent Analyses of Plume Rise
Observations, In Proceedings of the Second
International Clean Air Congress, Academic Press, New
York.
- Briggs, G.A., 1972: Discussion on Chimney Plumes in
Neutral and Stable Surroundings. Atmos. Environ., 6,
507-510.
- Briggs, G.A., 1974: Diffusion Estimation for Small
Emissions. In ERL, ARL USAEC Report ATDL-106. U.S.
Atomic Energy Commission, Oak Ridge, Tennessee.
- Briggs, G.A., 1975: Plume Rise Predications. In Lectures
on Air Pollution and Environmental Impact Analysis,
American Meteorological Society, Boston,
Massachusetts.
- Byun, D.W. and R. Dennis, 1995: Design Artifacts in
Eulerian Air Quality Models: Evaluation of the
Effects of Layer Thickness and Vertical Profile
Correction on Surface Ozone Concentrations. Atmos.
Environ., 29, 105-126.

Chico, T. and J.A. Catalano, 1986: Addendum to the User's Guide for MPTER. Contract No. EPA 68-02-4106, U.S. Environmental Protection Agency, Research Triangle Park, North Carolina 27711.

Cramer, H.E., et al., 1972: Development of Dosage Models and Concepts. Final Report Under Contract DAAD09-67-C-0020(R) with the U.S. Army, Desert Test Center Report DTC-TR-609, Fort Douglas, Utah.

Dumbauld, R.K. and J.R. Bjorklund, 1975: NASA/MSFC Multilayer Diffusion Models and Computer Programs -- Version 5. NASA Contractor Report No. NASA CR-2631, National Aeronautics and Space Administration, George C. Marshall Space Center, Alabama.

Dyer, A.J., 1974: A review of flux-profile relationships. Boundary-Layer Meteorol., 7, 363-372.

Environmental Protection Agency, 1985: Guideline for Determination of Good Engineering Practice Stack Height (Technical Support Document for the Stack Height Regulations) - Revised, EPA-450/4-80-023R, U.S. Environmental Protection Agency, Research Triangle Park, NC 27711. (NTIS No. PB 85-225241)

Environmental Protection Agency, 1992. Comparison of a Revised Area Source Algorithm for the Industrial Source Complex Short Term Model and Wind Tunnel Data. EPA Publication No. EPA-454/R-92-014. U.S. Environmental Protection Agency, Research Triangle Park, NC. (NTIS No. PB 93-226751)

Environmental Protection Agency, 1992. Sensitivity Analysis of a Revised Area Source Algorithm for the Industrial Source Complex Short Term Model. EPA Publication No. EPA-454/R-92-015. U.S. Environmental Protection Agency, Research Triangle Park, NC. (NTIS No. PB 93-226769)

Environmental Protection Agency, 1992. Development and Evaluation of a Revised Area Source Algorithm for the Industrial Source Complex Long Term Model. EPA

Publication No. EPA-454/R-92-016. U.S. Environmental Protection Agency, Research Triangle Park, NC. (NTIS No. PB 93-226777)

Environmental Protection Agency, 1994. Development and Testing of a Dry Deposition Algorithm (Revised). EPA Publication No. EPA-454/R-94-015. U.S. Environmental Protection Agency, Research Triangle Park, NC. (NTIS No. PB 94-183100)

Gifford, F.A., Jr. 1976: Turbulent Diffusion - Typing Schemes: A Review. Nucl. Saf., 17, 68-86.

Hicks, B.B., 1982: Critical assessment document on acid deposition. ATDL Contrib. File No. 81/24, Atmos. Turb. and Diff. Laboratory, Oak Ridge, TN.

Holzworth, G.C., 1972: Mixing Heights, Wind Speeds and Potential for Urban Air Pollution Throughout the Contiguous United States. Publication No. AP-101, U.S. Environmental Protection Agency, Research Triangle Park, North Carolina 27711.

Horst, T.W., 1983: A correction to the Gaussian source-depletion model. In Precipitation Scavenging, Dry Deposition and Resuspension, H.R. Pruppacher, R.G. Semonin, W.G.N. Slinn, eds., Elsevier, NY.

Huber, A.H. and W.H. Snyder, 1976: Building Wake Effects on Short Stack Effluents. Preprint Volume for the Third Symposium on Atmospheric Diffusion and Air Quality, American Meteorological Society, Boston, Massachusetts.

Huber, A.H. and W.H. Snyder, 1982. Wind tunnel investigation of the effects of a rectangular-shaped building on dispersion of effluents from short adjacent stacks. Atmos. Environ., 176, 2837-2848.

Huber, A.H., 1977: Incorporating Building/Terrain Wake Effects on Stack Effluents. Preprint Volume for the Joint Conference on Applications of Air Pollution

Meteorology, American Meteorological Society, Boston, Massachusetts.

Jindal, M. and D. Heinold, 1991: Development of particulate scavenging coefficients to model wet deposition from industrial combustion sources. Paper 91-59.7, 84th Annual Meeting - Exhibition of AWMA, Vancouver, BC, June 16-21, 1991.

McDonald, J.E., 1960: An Aid to Computation of Terminal Fall Velocities of Spheres. J. Met., 17, 463.

McElroy, J.L. and F. Pooler, 1968: The St. Louis Dispersion Study. U.S. Public Health Service, National Air Pollution Control Administration, Report AP-53.

National Climatic Center, 1970: Card Deck 144 WBAN Hourly Surface Observations Reference Manual 1970, Available from the National Climatic Data Center, Asheville, North Carolina 28801.

Pasquill, F., 1976: Atmospheric Dispersion Parameters in Gaussian Plume Modeling. Part II. Possible Requirements for Change in the Turner Workbook Values. EPA-600/4-76-030b, U.S. Environmental Protection Agency, Research Triangle Park, North Carolina 27711.

Perry, S.G., R.S. Thompson, and W.B. Petersen, 1994: Considerations for Modeling Small-Particulate Impacts from Surface Coal Mining Operations Based on Wind-Tunnel Simulations. Proceedings Eighth Joint Conference on Applications of Air Pollution Meteorology, January 23-28, Nashville, TN.

Petersen, W.B. and E.D. Rumsey, 1987: User's Guide for PAL 2.0 - A Gaussian-Plume Algorithm for Point, Area, and Line Sources, EPA/600/8-87/009, U.S. Environmental Protection Agency, Research Triangle Park, North Carolina.

Pleim, J., A. Venkatram and R. Yamartino, 1984: ADOM/TADAP model development program. Volume 4. The dry

deposition module. Ontario Ministry of the Environment, Rexdale, Ontario.

- Press, W., B. Flannery, S. Teukolsky, and W. Vetterling, 1986: Numerical Recipes, Cambridge University Press, New York, 797 pp.
- Schulman, L.L. and S.R. Hanna, 1986: Evaluation of Downwash Modifications to the Industrial Source Complex Model. J. Air Poll. Control Assoc., 36 (3), 258-264.
- Schulman, L.L. and J.S. Scire, 1980: Buoyant Line and Point Source (BLP) Dispersion Model User's Guide. Document P-7304B, Environmental Research and Technology, Inc., Concord, MA.
- Scire, J.S. and L.L. Schulman, 1980: Modeling Plume Rise from Low-Level Buoyant Line and Point Sources. Proceedings Second Joint Conference on Applications of Air Pollution Meteorology, 24-28 March, New Orleans, LA. 133-139.
- Scire, J.S., D.G. Strimaitis and R.J. Yamartino, 1990: Model formulation and user's guide for the CALPUFF dispersion model. Sigma Research Corp., Concord, MA.
- Slinn, W.G.N., 1982: Predictions for particle deposition to vegetative canopies. Atmos. Environ., 16, 1785-1794.
- Slinn, S.A. and W.G.N. Slinn, 1980: Predictions for particle deposition and natural waters. Atmos. Environ., 14, 1013-1016.
- Thompson, R.S., 1994: Residence Time of Contaminants Released in Surface Coal Mines -- A Wind Tunnel Study. Proceedings Eighth Joint Conference on Applications of Air Pollution Meteorology, January 23-28, Nashville, TN.

Touma, J.S., J.S. Irwin, J.A. Tikvart, and C.T. Coulter, 1995. A Review of Procedures for Updating Air Quality Modeling Techniques for Regulatory Modeling Programs. J. App. Meteor., 34, 731-737.

Turner, D.B., 1970: Workbook of Atmospheric Dispersion Estimates. PHS Publication No. 999-AP-26. U.S. Department of Health, Education and Welfare, National Air Pollution Control Administration, Cincinnati, Ohio.

Venkatram, A., 1988: A Simple Model for Dry Deposition and Particle Settling. Subcontractor Progress Report 2 (including addendum), EPA Contract No. 68D70002, Work Assignment No. 1-001.

Yamartino, R.J., J.S. Scire, S.R. Hanna, G.R. Carmichael and Y.S. Chang, 1992: The CALGRID mesoscale photochemical grid model. Volume I. Model formulation. Atmos. Environ., 26A, 1493-1512.

INDEX

Area source
 deposition algorithm 1-60, 2-14
 for the Long Term model 2-8, 2-9
 for the Short Term model 1-40, 1-44
 Atmospheric resistance 1-56
 Attenuation correction factor
 in complex terrain 1-69
 Briggs plume rise formulas
 buoyant plume rise 1-7, 1-9
 momentum plume rise 1-8, 1-10
 stack tip downwash 1-6
 Building downwash procedures 1-24, 2-5
 and buoyancy-induced dispersion 1-31
 effects on dispersion parameters 1-21
 for the Long Term model 1-64, 2-2, 2-4, 2-5
 general 1-5, 1-22
 Huber and Snyder 1-23
 Schulman and Scire 1-5, 1-12, 1-28, 1-29
 Schulman-Scire plume rise 1-12, 1-14
 virtual distances 1-20
 wake plume height 1-12
 Buoyancy flux 1-6, 1-14
 Buoyancy-induced dispersion 1-30, 1-31, 2-6
 Buoyant plume rise
 stable 1-9
 unstable and neutral 1-7
 Cartesian receptor network 1-3
 Complex terrain modeling
 Short Term model 1-63, 1-72
 Crossover temperature difference 1-7
 Crosswind distance 1-2, 1-3, 1-4, 1-64, 1-65, 2-4
 Decay coefficient 1-40
 Decay term 1-3, 1-39, 1-65
 for the Long Term model 1-65, 2-3, 2-7
 for the Short Term model 1-39, 1-69

Depletion
 for the dry deposition algorithm 1-39
 for the wet deposition algorithm 1-61
 Deposition velocity 1-35, 1-54
 Direction-specific building dimensions 1-22, 1-29
 with Huber-Snyder downwash 1-29
 Dispersion coefficients
 see Dispersion parameters 1-15, 1-66
 Dispersion parameters
 for the Long Term model 2-4
 McElroy-Pooler 1-15, 1-19
 Pasquill-Gifford 1-15, 1-16, 1-17, 1-18
 Distance-dependent plume rise 1-13
 Downwind distance 1-2, 1-3, 1-4, 1-64, 1-65, 2-4
 and virtual distance 1-20
 for area sources 1-44
 for building wake dispersion 1-24
 for dispersion coefficients 1-15
 Dry deposition 1-3, 1-65, 2-12
 for the Long Term model 2-12
 for the Short Term model 1-53
 Elevated terrain 1-34, 1-67, 2-7
 truncation above stack height 1-34
 Entrainment coefficient 1-14
 Final plume rise 1-30
 distance to 1-7
 stable 1-9, 1-10
 unstable or neutral 1-7, 1-8
 Flagpole receptor 1-32
 Gaussian plume model 1-2, 1-63
 sector averages for complex terrain 1-63
 sector averages for Long Term 2-1
 GEP stack height 1-12, 1-30
 Gradual plume rise 1-10
 for buoyant plumes 1-10
 for Schulman-Scire downwash 1-13, 1-14
 stable momentum 1-11

unstable and neutral momentum 1-11
 used for wake plume height 1-12
 Half life 1-40
 Huber-Snyder downwash algorithm 1-5
 Initial lateral dimension
 for the Long Term model 2-5
 for volume sources 1-42, 1-43
 Initial plume length
 Schulman-Scire downwash 1-13
 Initial plume radius
 Schulman-Scire downwash 1-13
 Initial vertical dimension
 for volume sources 1-43
 Intermediate terrain 1-72
 Jet entrainment coefficient 1-11, 1-14
 Lateral dispersion parameters 1-16, 1-19, 1-30
 for the Long Term model 2-4
 Lateral virtual distance
 for the Long Term model 1-64, 2-3, 2-4
 Lateral virtual distances
 for building downwash 1-26
 Line source
 approximation for Schulman-Scire sources 1-13
 Line sources, modeled as volumes 1-40, 1-42, 1-43, 2-8
 Linear decay factor
 Schulman-Scire downwash 1-13, 1-29
 Long-term dispersion model 2-1
 McElroy-Pooler dispersion parameters
 see Dispersion parameters 1-19
 Mixing heights 1-33
 Momentum flux 1-6, 1-14
 Momentum plume rise 1-11, 1-23, 1-29
 stable 1-10
 unstable and neutral 1-8
 Open pit source
 deposition algorithm 1-60, 2-14
 for the Long Term model 2-12

for the Short Term model 1-48
 Open pit sources 1-41, 1-48
 Pasquill-Gifford dispersion parameters
 see Dispersion parameters 1-16
 Plume rise
 for Schulman-Scire downwash 1-12
 for the Long Term model 2-4
 for the Short Term model 1-5, 1-65
 Point source
 deposition algorithm 1-59, 2-13
 dispersion parameters 1-15, 2-4
 for the Long Term model 2-1
 for the Short Term model 1-2
 Polar receptor network 1-3
 Receptors
 calculation of source-receptor distances 1-3, 1-4
 Rural
 dispersion parameters 1-15
 virtual distances 1-20, 1-25
 Schulman-Scire downwash algorithm 1-5
 Short-term dispersion model 1-1
 Sigma-y 1-15, 1-66
 Sigma-z 1-15, 1-66
 Smoothing function
 for the Long Term model 2-3, 2-7
 Stability parameter 1-9, 1-14
 Stack-tip downwash 1-6
 for wake plume height 1-12
 Uniform vertical mixing 1-32
 Urban
 decay term for SO₂ 1-40
 dispersion parameters 1-15
 virtual distances 1-20, 1-26
 Vertical dispersion parameters 1-17, 1-18, 1-19
 Vertical term 1-3, 1-45, 1-65, 2-6
 for gases and small particulates 1-31
 for large particulates 2-7

for the Long Term model 1-65, 2-3, 2-6
for the Short Term model 1-31, 1-67
for uniform vertical mixing 1-32, 1-33
in complex terrain 1-67
in elevated terrain 1-34, 2-7
Vertical virtual distances
for building downwash 1-25, 1-26
Virtual distances . . . 1-20, 1-21, 1-28, 1-29, 1-41, 1-45
for the Long Term model 2-4, 2-5
for volume sources 1-41
Virtual point source 1-41, 1-64, 2-2, 2-8, 2-9
Volume source 1-43
deposition algorithm 1-59, 2-13
for the Long Term model 2-8
for the Short Term model 1-40, 1-41
Wet deposition
for the Short Term model 1-61
Wind speed
minimum wind speed for modeling 1-5
Wind speed profile 1-4, 1-65, 2-4